

Original Research

Phyto-Fabrication *Tribulus terrestris* Mediated Iron Oxide Nanoparticles: A Promising Approach of Antioxidant and Anticancer Activities via *in vitro* and *in silico* Studies

Ranjani Renugopal¹, Thirunavukkarasu Palaniyandi^{1,2,*}, Barani Kumar Rajendran³, Senthilkumar Kaliamoorthy⁴, Maddaly Ravi⁵, Gomathy Baskar¹, Mugip Rahaman Abdul Wahab¹, Hemapreethi Surendran¹, Mahalakshmi Nannan⁶, Manojkumar Govindaraj⁷, Asha Sivaji⁸, Wahidah H. Al-Qahtani⁹, Rashid Ayub⁹

Academic Editor: Sukmook Lee

Submitted: 7 June 2024 Revised: 21 October 2024 Accepted: 31 October 2024 Published: 30 May 2025

Abstract

Background: Plant-mediated iron nanoparticles are increasingly utilized in biomedical and health applications due to their biocompatibility and nontoxicity. The therapeutic characteristics of these nanoparticles are extensively diverse. Methods: In this study, iron nanoparticles synthesized from Tribulus terrestris were characterized using various techniques, including Fourier transform infrared (FTIR) spectroscopy, scanning electron microscopy (SEM), transmission electron microscopy (TEM), UV-visible spectroscopy, vibrating sample magnetometry (VSM), and X-ray diffraction (XRD) analysis. Antioxidant properties were assessed using the hydrogen peroxide (H2O2) and 2, 2-diphenyl-1-picrylhydrazyl (DPPH) assays. Anti-inflammatory activity was evaluated through protein denaturation studies. Antimicrobial activity was tested against wound pathogens. The effects of anticancer and wound healing were investigated using HCT-116 (colon cancer) and MG-63 (osteosarcoma) cells. Molecular docking studies were performed to assess the binding affinity of Tribulus terrestris bioactive compounds with proteins involved in the Adenomatous polyposis coli (APC) pathway of colon cancer. Results: The Tribulus terrestris-mediated Fe₃O₄ nanoparticles exhibited a peak at 290 nm using UV-visible spectroscopy. SEM and TEM analyses revealed that the nanoparticles were aggregated with an average size of 29 ± 0.24 nm. XRD analysis indicated a cubic crystalline structure. FTIR spectroscopy identified the biomolecules involved in the synthesis, and VSM confirmed a magnetic saturation of 14.75 emu/g. The antioxidant activity was demonstrated with DPPH (65.5%) and hydrogen peroxide (65.56%) assays at a dosage of 50 µg/mL, demonstrating a significant inhibition. The protein denaturation assay revealed a maximum inhibition of 54.57%. Lactobacillus had the strongest antibacterial activity at a concentration of 100 µg/mL, with an inhibitory zone of 35 mm. The anticancer assays showed IC₅₀ values of 25.95 µg/mL for colon cancer (HCT-116) and 35.36 µg/mL for osteosarcoma (MG-63), indicating significant cytotoxicity, particularly against colon cancer cells. The nanoparticles also demonstrated effective regulation of cell migration at 50 µg/mL. Molecular docking studies revealed strong binding affinities between Tribulus terrestris compounds and APC pathway proteins relevant to colon cancer. Conclusion: This research underscores the potential of Tribulus terrestris-mediated iron nanoparticles as a sustainable and eco-friendly approach with significant antioxidant and anticancer properties, especially in combating colon cancer. The findings highlight their effectiveness in reducing oxidative stress, inhibiting cancer cell proliferation, and enhancing wound healing.

Keywords: Tribulus terrestris; iron nanoparticles; antibacterial; antioxidant; anticancer; colon cancer; molecular docking; osteosarcoma

1. Introduction

Cancer is characterized by uncontrolled cell proliferation caused by oncogenic signals that occur at an incorrect time and location [1]. Mutations in the DNA sequence of cancer cell genomes cause all malignancies [2]. Colon and bone cancer is one of the most common cancers, which leads to the highest mortality rate worldwide. Early detec-

tion of colon and bone cancer makes them extremely treatable and frequently curable with conventional therapy [3], but at the metastatic stage, it's not treatable, and also treatments contain major obstacles like balancing treatment toxicity with quality and the high cost of disposing of chemical waste sludge, lack of therapeutic target, the resulting production of toxic metabolites, and the expense of operation.

¹Department of Biotechnology, Dr. M.G.R Educational and Research Institute, 600 095 Chennai, Tamil Nadu, India

²ACS-Advanced Medical Research Institute, Dr. M.G.R Educational and Research Institute, Maduravoyal, 600095 Chennai, Tamil Nadu, India

³Yale School of Medicine, Yale University, New Haven, CT 06510, USA

⁴Department of Electronics and Communication Engineering, Dr. M.G.R Educational and Research Institute, 600 095 Chennai, Tamil Nadu, India

⁵Department of Human Genetics, Sri Ramachandra Institute of Higher Education and Research, Porur, 600116 Chennai, Tamil Nadu, India

⁶Department of Genetic Engineering, School of Bioengineering, SRM Institute of Sciences and Technology, Kattankulathur, 603 203 Chengalpattu, Tamil Nadu, India

⁷PG & Research Department of Microbiology and Biotechnology, Presidency College, 600005 Chennai, Tamil Nadu, India

⁸Department of Biochemistry, DKM College for Women, 632001 Vellore, Tamil Nadu, India

⁹Department of Food Sciences & Nutrition, College of Food & Agriculture Sciences, King Saud University, 11451 Riyadh, Saudi Arabia

^{*} Correspondence: ppthirunacas@gmail.com; thirunavukkarasu.ibt@drmgrdu.ac.in (Thirunavukkarasu Palaniyandi)

Hence, to get over these obstacles, researchers have studied the use of nanotechnology in cancer detection and therapy [4].

Nanotechnology is one of the most well-known multidisciplinary fields and a new area of technology that has enormous promise to provide ground-breaking discoveries with practical applications including physics, chemistry, biology, medicine, informatics, and engineering [5,6]. The key characteristic of nanotechnology is its capacity to generate huge structures with essentially novel molecular organization at the molecular level, atom by atom [7]. Nanoparticles are a general term for materials having a minimum size of less than 100 nm, and they are a byproduct of nanotechnology [8]. Their atomic, electronic, and magnetic structures, physical and chemical characteristics, and reactivity about the bulk material are all significantly altered by the small number of atoms in the particles and the significant fraction of atoms that are at or near surfaces [9]. Concerns for the production of nanomaterials include social adaptation, environmental sustainability, and economic feasibility in addition to the availability of local resources [10,11].

In silico approaches are advantageous for the investigation of the pharmacology of potential therapeutics through the use of computer-simulated models and for the development of biomedicines. The pharmaceutical industry has used in in silico methods for decades to find small molecules that can modulate the function of an identified target protein and thereby modulate the disease phenotype [12]. Iron oxide nanoparticles (Fe₃O₄-NPs) synthesised using Tribulus terrestris (T. terrestris) were evaluated using in vitro tests to determine their antimicrobial and cytotoxic effects. Compared to the Tribulus terrestris extract, T. terrestris-mediated iron nanoparticles demonstrated superior in vivo and in vitro results. This improvement is attributed to the active phytochemicals in the plant, which contribute significantly to the observed effects, as noted by Kaushik et al. [13].

Fe₃O₄ nanoparticles (Fe₃O₄-NPs) vary by their distinctive optical, electrical, antibacterial, and catalytic properties. The synthesis of iron NPs represents a significant advancement in nanomaterial due to their accessibility, relative affordability, and low toxicity [14,15]. Plant-based pharmaceuticals continue to be a major source of therapeutic molecules. Consequently, Fe₃O₄-NPs have broad applications across various sectors, including biomedicine, bioremediation, engineering, cosmetics, and clinical materials [16,17]. They are increasingly recognized as promising options for cancer treatment [18].

Tribulus terrestris exhibits a range of pharmacological activities, including effects on the central nervous system, anti-urolithiasis, aphrodisiac properties, cardiac health, antibacterial action, hepatoprotection, analgesic effects, antispasmodic properties, anticancer activity, anthelmintic properties, larvicidal effects, diuretic action, and

anti-cariogenic properties [19,20]. Plants with anti-cancer properties primarily act by inhibiting cancer-promoting enzymes, repairing DNA, promoting the synthesis of antitumor enzymes, boosting immunity, and providing antioxidant effects without harming healthy human cells [21,22]. *Tribulus terrestris* is particularly rich in spirostanol and furostanol saponins, with diosgenin being a key spirostanol sapogenin. Measuring diosgenin is crucial for the quality control of *T. terrestris*, which also has potent antilithiatic activity demonstrated by *in vitro* and *in vivo* studies [23].

When combined with herbal treatments, nanomedicines can deliver drugs specifically to the target site, minimizing effects on healthy cells, stomach acidity, liver metabolism, and blood circulation. Their small size also extends the duration of the drug's presence in the bloodstream [24]. Iron nanoparticles are increasingly emphasized for their role in diagnostics and drug delivery, particularly in cancer treatment, where they enhance the efficacy of primary irradiation. Magnetic orientation ensures that magnetic particles reach the tumor site, potentially having a significant anticancer effect [12].

This is the first study to demonstrate that iron nanoparticles (Tt-Fe₃O₄-NPs) produced from the aerial parts of *T. terrestris* are effective against colon cancer cells. The research investigated Fe₃O₄-NPs biosynthesized from *T. terrestris* aerial parts using *in vitro* and *in silico* methods. Notably, *Tribulus*-Fe₃O₄-NPs were found to be more effective against colon cancer cells than bone cancer cells at lower concentrations.

2. Materials and Methods

2.1 Sample Collection

Tribulus terrestris (Tt) was used in this study. It is a flowering plant with yellow flowers and is included in numerous traditional medicine formulations. The plant was collected from Pudhur and its surrounding areas in Chennai. It was identified as 387.1753 and authenticated by the Siddha Central Research Institute in Chennai.

2.2 Preparation of Plant Extract

The aerial parts of the plant were washed and cleaned with distilled water, then cut into small pieces, shade-dried, and finally powdered. This powder was used in the synthesis of nanoparticles [25].

2.3 Synthesis of Iron Oxide Nanoparticles

A beaker containing 100 mL of deionized water and 1g of powdered plant material was heated at 60 °C for 30 minutes. The extract was then stored at ambient temperature, cooled, and filtered through Whatman filter paper. Fe₃O₄-NPs were synthesized from the filtrate. In a conical flask, 50 mL of the extract was mixed with 50 mL of ferric chloride and stirred for 20 minutes using a magnetic stirrer. The reaction mixture was continuously stirred to produce



Fe₃O₄-NPs. The appearance of a black color indicated the formation of nanoparticles [26].

2.4 Chemicals Used

Ascorbic acid (vitamin C), Antibiotic-antimycotic solution, Bovine Serum Albumin (BSA), FeCl₃ (ferric chloride), Hydrogen peroxide (H₂O₂), 2,2-Diphenyl-1-picrylhydrazyl (DPPH) were purchased from HiMedia, India. Methyl Thiazole Tetrazolium (MTT) salt, trypsin-EDTA, Dulbecco's Modified Eagle Medium (DMEM), and 100× Phosphate-buffered saline (PBS) were purchased from Gibco, Thermo Scientific, India [26].

2.5 Characterization of Iron Oxide Nanoparticles

The optical characteristics of the nanoparticles were examined using UV-visible spectroscopy (Shimadzu, Kyoto, Japan). The synthesised Fe₃O₄-NPs were analyzed in this work by identifying their highest absorption peak within a particular wavelength range of 200–700 nm [27]. Fourier-transform infrared spectroscopy (FTIR) (IR Prestige 21, Shimadzu, Kyoto, Japan) was used to analyze the functional groups of the iron oxide nanoparticles with scan rates between 400 and 4000 cm⁻¹ were used for this analysis [28]. X-ray diffraction (XRD) (PANalytical, Almelo, Netherlands) patterns were utilized to determine the crystal structure of the nanoparticles [29]. Scanning electron microscopy (SEM) (FEI, Quanta 200, Hillsboro, OR, USA) [30] and transmission electron microscopy (TEM) (JEOL Japan, JEM-2100 plus) [31] provided information on the size and morphology of the nanoparticles. The magnetic properties, including magnitude and direction of the magnetic field, were assessed using a vibrating sample magnetometer (VSM) [32].

2.6 Antioxidant Activity

2.6.1 DPPH Radical Scavenging Activity

The DPPH radical scavenging activity of *Tribulus*-Fe₃O₄-NPs and ascorbic acid was evaluated using a standard method. Test samples and standard ascorbic acid at varying concentrations (10–50 μ g/mL) were mixed with DPPH (1 mL of 0.1 mM) diluted in 50% ethanol. The reaction mixture was incubated for 30 minutes and then measured spectrophotometrically at 517 nm [33].

Percentage of Inhibition = $[(Ab - As) / Ab] \times 100$ where Ab = absorbance of the blank and As = absorbance of the test samples.

2.6.2 H₂O₂ Scavenging Activity

The scavenging activity of vitamin C and *Tribulus*-Fe₃O₄-NPs against hydrogen peroxide was tested. Phosphate buffer was added to an aqueous solution of 40 mM hydrogen peroxide (pH 7.4). A 0.6 mL solution of hydrogen peroxide containing standard and test samples at concentrations (10, 20, 30, 40, and 50 μg/mL) was prepared.

The mixture was analyzed spectrophotometrically at 230 nm after a 10-minute incubation period [34].

Percentage of Inhibition = $[(Ab - As) / Ab] \times 100$ where Ab = absorbance of the blank and As = absorbance of the test samples.

2.7 Anti-Inflammatory Activity

The protein denaturation assay was conducted using the method outlined by Sultana *et al.* [35]. The reaction mixture (5 mL) consisted of 0.02 mL of extract, 4.78 mL of phosphate-buffered saline (PBS, pH 6.4), and 0.2 mL of 1% bovine serum albumin. After incubation at 37 °C for 15 minutes, the mixture was heated to 70 °C for 5 minutes and then cooled. The intensity of protein denaturation was measured at 660 nm using a UV-visible spectrometer. The control solution was phosphate buffer. The percentage of inhibition was calculated as follows:

Percentage of Inhibition = $[(Ab - As) / Ab] \times 100$ where Ab = absorbance of the control sample and As = absorbance of the test samples.

2.8 Antibacterial Activity

The antibacterial activity of *Tribulus*-Fe $_3$ O $_4$ -NPs was evaluated using the agar well diffusion technique. Bacterial cultures of *Lactobacillus, Vibrio cholerae, Staphylococcus aureus,* and *Pseudomonas aeruginosa* were maintained in nutrient broth. A 24-hour bacterial culture was used to swab Muller Hinton agar plates. Wells (6 mm in diameter) were punched into the agar plates, and 25 μ L, 50 μ L, and 100 μ L of the green-synthesized Fe $_3$ O $_4$ -NPs were added to each well, along with 30 μ L of a control antibiotic. The plates were incubated at 37 °C for 24 hours, and the zone of inhibition around the wells was measured [36].

2.9 Anticancer Activity

2.9.1 Maintenance of Cancer Cell Lines

Anticancer drug testing was conducted using human colorectal cancer (HCT-116) and bone cancer (MG-63) cells. Cell lines were obtained from the National Centre for Cell Science (NCCS) in Pune, India, and cultured in T-25 flasks with DMEM medium. The medium was supplemented with antimitotic solution (1%), fetal bovine serum (10%) and antibiotics. The flasks were maintained in an incubator (37 °C) with 5% carbon dioxide (CO₂) and monitored regularly [37]. Cell lines were validated by short tandem repeat (STR) profiling and tested negative for mycoplasma. Cells were all cultured in a humidified incubator at 37 °C and 5% CO₂.

2.9.2 Cytotoxic Activity of Tt-Fe₃O₄-NPs

The cytotoxicity of *Tribulus*-Fe $_3$ O $_4$ -NPs was tested against colorectal cancer (HCT-116) and bone cancer (MG-63) cells. Cells were plated into 96-well plates at a density of 4 \times 10 5 cells per well and incubated for 24 hours. Fresh wells with varying amounts of *Tribulus*-Fe $_3$ O $_4$ -NPs (3 to



 $50 \mu g/mL$) were added. After 24 hours, the media was discarded and $100 \mu L$ of MTT solution (5 mg/mL) was added to each well. The plate was incubated for 4 hours. Viable cells were indicated by the formation of purple formazan crystals. After dissolving the crystals in $100 \mu L$ of dimethyl sulfoxide (DMSO), the optical density at 540 nm was measured using an ELISA plate reader [38].

2.10 Wound Healing Assay

In a 6-well plate, 7.5×10^4 colon cancer cells were seeded per well and allowed to grow. A scratch was made using micropipette tips (10 μ L). *Tribulus*-Fe₃O₄-NPs were applied to the scratched cells at concentrations of 10, 25, and 50 μ g/mL. An untreated well served as a control. The cells were rinsed with 1.5 mL of PBS and incubated in a CO₂ incubator [39].

2.11 Molecular Docking and in Silico Analysis

Molecular docking predicts ligand-protein interactions and is widely used in structural biology and drug development. Protein-ligand interactions are crucial for structure-based drug design and protein function prediction, as noted by Naqvi *et al.* [40]. PyrX virtual screening tool version 0.8 (https://sourceforge.net/projects/pyrx/) was used for virtual docking, and Discovery Studio was used for interaction analysis.

2.11.1 Ligand File Preparation

Docking small molecule compounds into receptor binding sites and determining the binding affinity of the complex are essential steps in drug development. Ibrahim *et al.* [41] conducted a GC/MS study of *Tribulus terrestris* fractions, identifying bioactive substances in the plant's methanol extract. These substances were selected as ligands for docking studies. The chosen compounds are stearic acid (CID: 5281), 2-hexanol, 2-methyl (CID: 12240), hexadecanoic acid (CID: 8181), octadecanoic acid (CID: 8201), 2-pentadecanone (CID: 10408), coumaric acid (CID: 323), benzofuran (CID: 10329), arachidic acid (CID: 444899), and 5FU (CID: 3385). The PyMOL program 3.0.4 (Schrödinger, Inc. New York, NY, USA) was used to convert ligand structures into PDB (Protein Data Bank) format for docking studies.

2.11.2 Protein File Preparation

Proteins involved in the APC pathway were selected for computational docking based on their role in colon cancer development. Proteins were obtained from the RCSB PDB collection. The selected proteins are KRT8 (PDB ID: P05787), TFRC (PDB ID: 3KAS), KLK6 (PDB ID: 1LO6), C3AR1 (PDB ID: 81A8), AHSG (PDB ID: P02765), GRP (PDB ID: 7W3Z), APOC1 (PDB ID: 6DVU), and CAV1 (PDB ID: Q03135). Ligands and water molecules were removed, and hydrogen bonds were added to upgrade the structures for docking studies [42].

2.11.3 Active Site Prediction

Active sites of the proteins were predicted using the Castp server. The PDB file was converted, and findings were used to predict active sites. The grid box dimensions for docking studies were set by condensing residues associated with these active sites in PyRx tools [42].

2.12 Statistical Analysis

Statistical analysis was performed using Microsoft Excel 2019 (Redmond, Washington, United States) to calculate standard deviation (SD) and compare test and control sample results. Results were considered statistically significant when the *p* value was less than 0.05 [42].





Fig. 1. Synthesis of *T. terrestris*-mediated iron nanoparticles.(A) Before colour change, (B) After colour change.

3. Results and Discussion

3.1 Synthesis of Iron Oxide Nanoparticles

The synthesis of iron nanoparticles was indicated by an immediate change in solution color and a decrease in pH after 1 hour of incubation when plant extract was added to the aqueous FeCl₃ solution. The reaction between ferric chloride and Tribulus terrestris aerial extract resulted in a color change from pale orange to dark brown (Fig. 1A,B). This color alter indicates that iron oxide nanoparticles (FeO) are being produced in solution as a result of the reduction of ferric ions (Fe₃+). Ferric chloride solution addition of effects, such as stabilization of the nanoparticles and a reduction in Fe₃+. Fe₃O₄-NPs synthesized from tribulus, were examined for absorption spectrum in the range of 200-800 nm wavelength. Periodically, the biosynthesized Fe₃O₄-NPs were initially, not shown any noticeable peaks. The synthesized *T. terrestris*-mediated iron nanoparticles (Tt-Fe₃O₄-NPs) showed a clear peak at 290 nm after the incubation of 30 minutes, shown in Fig. 2. Similar results were observed in previous studies, including the synthesis of Fe₃O₄-NPs from *Tribulus terrestris* leaves [43] and *Phyl*lanthus niruri plant leaf and fruit parts [44].



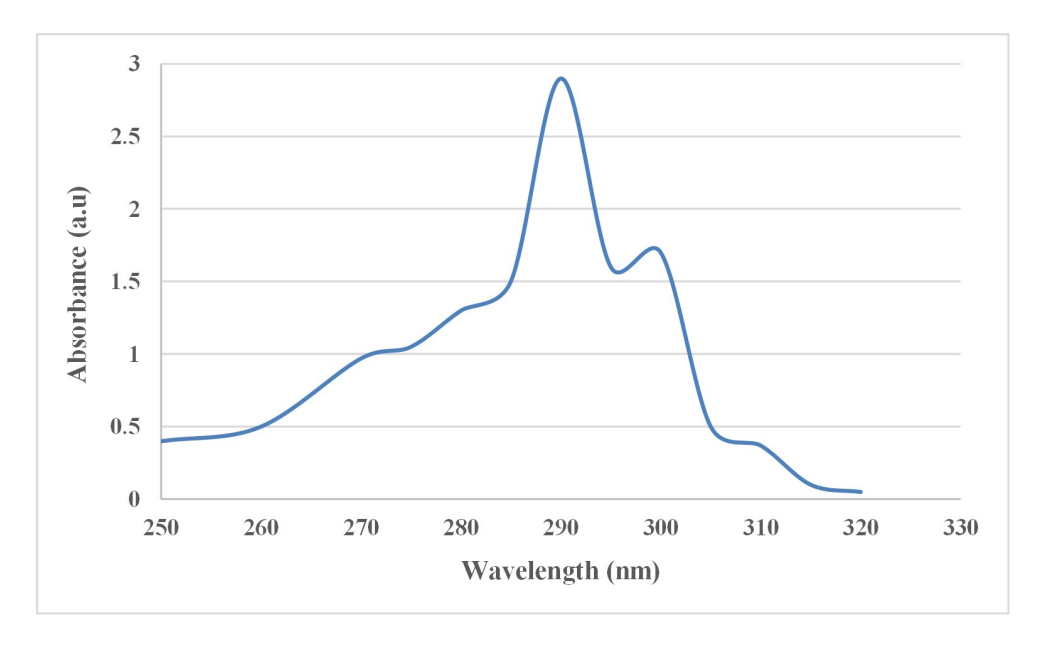


Fig. 2. UV-visible spectroscopy analysis of *T. terrestris*-mediated iron nanoparticles.

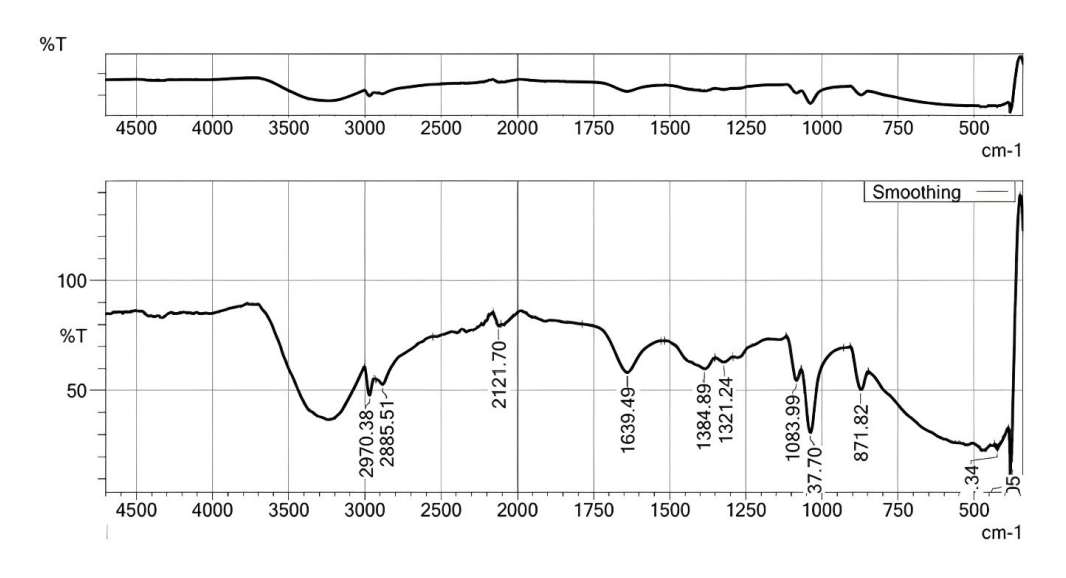


Fig. 3. FTIR spectra analysis of *T. terrestris*-mediated iron nanoparticles. FTIR, Fourier-transform infrared spectroscopy.

3.2 FTIR Analysis of T. terrestris-Fe₃O₄-NPs

FTIR spectroscopy was employed to identify the functional groups involved in the reduction of Fe₃O₄ nanoparticles by *Tribulus terrestris* and to determine the specific groups responsible for this process. The FTIR spectrum of the *T. terrestris* extract showed bands at 2970.80 cm⁻¹ and 2885.51 cm⁻¹, corresponding to the C-H stretching of alkanes, indicating the presence of alkane groups. Fig. 3 depicts additional bands at 2121.70 cm⁻¹ (N=N=N stretching, indicating azide groups), 1639.49 cm⁻¹ (C=C stretching of alkanes), 1384.89 cm⁻¹ (C-H bending of alkanes), 1321.24 cm⁻¹ (N-O stretching of nitro compounds), and 1038.99 cm⁻¹ (C-O stretching of primary alcohols). The broad and intense peak at 2970.38 cm⁻¹ suggests the presence of O-H stretching bonds from both alcohol and phenolic groups in the synthesized *T. terrestris*-Fe₃O₄-NPs.

Phenolic compounds in plant extracts are often attributed as the primary agents responsible for the reduction of Fe³⁺ to Fe⁰ [45]. Rajendran *et al.* [46] conducted FTIR analysis on iron oxide nanoparticles synthesized from *Sesbania grandiflora* (Agati) and observed a significant peak at 1650 cm⁻¹, corresponding to N-H bending, with a visible bandwidth spanning 1500–600 cm⁻¹. Similarly, Pallela *et al.* [47] identified functional groups in *Sida cordifolia* through FTIR spectroscopy, noting strong peaks around 2928 cm⁻¹ and 2429 cm⁻¹, which correspond to methyl and amine groups, respectively.

3.3 XRD Analysis of T. terrestris-Fe₃O₄-NPs

X-ray powder diffraction (XRD) was utilized to evaluate the crystalline structure and phase of the nanoparticles. The XRD pattern of iron oxide nanoparticles synthesized



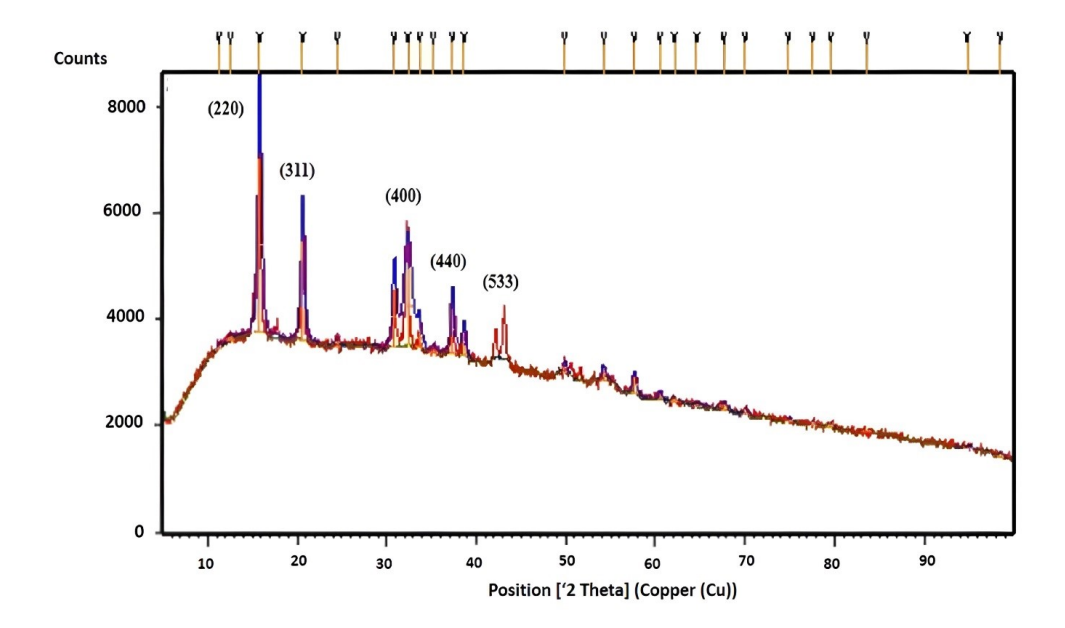


Fig. 4. XRD analysis of T. terrestris-mediated iron nanoparticles. XRD, X-ray diffraction.

from *Tribulus terrestris* (T. *terrestris*)-Fe₃O₄-NPs is shown in Fig. 4. The diffraction peaks observed at 15.96°, 20.67°, 32.31°, and 31.01° correspond to Bragg's reflections for the (220), (311), (400), (440), and (533), respectively. These peaks are consistent with the Fe₃O₄ nanoparticle data in the JCPDS database. Dhuper *et al.* [48] performed XRD analysis on *Mangifera indica*-mediated Fe₃O₄-NPs and found that the X-ray diffraction, using a graphite monochromator, revealed a rhombohedral crystalline structure with a wavelength of 1.54060 Å. Similarly, Patil *et al.* [49] reported that *Triadica procumbens*-mediated Fe₃O₄-NPs displayed peaks at 17.24°, 32.5°, and 39.06°, which corresponded to the (311) planes and confirmed the cubic structure of the nanoparticles.

3.4 SEM and TEM Analysis of T. terrestris-Fe₃O₄-NPs

Scanning Electron Microscopy (SEM) provides highresolution images of nanoparticles, revealing their size, shape, composition, electrical conductivity, topography, and surface features [50]. The SEM analysis of Tribulus terrestris-Fe₃O₄-NPs showed clusters of nanoparticles with an irregular spherical shape (Fig. 5A,B). Transmission Electron Microscopy (TEM) further revealed that the green-synthesized T. terrestris-Fe₃O₄ nanoparticles were predominantly spherical and exhibited accumulation. This morphology is attributed to the hydroxyl groups present in the plant extract. The nanocomposite was composed of iron and oxygen, with a mean diameter of 29 \pm 0.24 nm (Fig. 5C). Fig. 5D shows a histogram of newly synthesized Tt-Fe₃O₄-NPs with a mean diameter. In comparison, Baskar et al. [51] reported that Hypnea valentiae-mediated Fe₃O₄-NPs have a similar value analyzed by TEM analysis and exhibited rectangular shapes as observed by SEM analysis. Similarly, Naseem and Farrukh [52] analyzed

nanoparticles from *Lawsonia inermis* (henna) and found them to clump together, displaying a deformed hexagonal-like morphology. Kheshtzar *et al.* [53] evaluated nanoparticles produced from *Pinus eldarica* needles by TEM and observed that they were predominantly spherical with sizes ranging from 8 to 34 nm. *Jasminoides* leaf extract synthesized Fe-NPs were reported to be globular with a size of 21 nm.

3.5 Magnetic Characterization of T. terrestris-Fe₃O₄-NPs

A prominent method for determining the magnetic properties of materials is vibrating sample magnetometry (VSM). This method involves subjecting samples to a varying electromagnetic field to measure properties such as magnetic retentivity (Mr), coercivity (Hci), and saturation magnetization (Ms). The magnetic properties of *Tribulus terrestris*-mediated Fe₃O₄-NPs were evaluated using VSM. Fig. 6 illustrates the magnetic behavior of these nanoparticles. The Fe₃O₄-NPs showed a saturation magnetization (Ms) of 14.75 emu/g, a coercivity (Hci) of 285.28 Oe and a magnetic retentivity (Mr) of 1.0244×10^{-6} emu/g.

Mahdavi et al. [54] studied the magnetic properties of Fe₃O₄-NPs synthesized from Sargassum muticum extract. These nanoparticles exhibited superparamagnetic behavior with a saturation magnetization of 22.1 emu/g, a coercivity of 82.3 Oe, and no remanence, indicating the presence of a single magnetic domain. Similarly, Izadiyan et al. [55] reported high saturation magnetization in iron oxide nanoparticles obtained from Juglans regia. These nanoparticles displayed a high saturation magnetization of 53.32 emu/g and a low coercivity of 32.50 Oe. The magnetization curves confirmed the high saturation magnetization and low coercivity characteristics of the J. regia-derived iron oxide NPs.



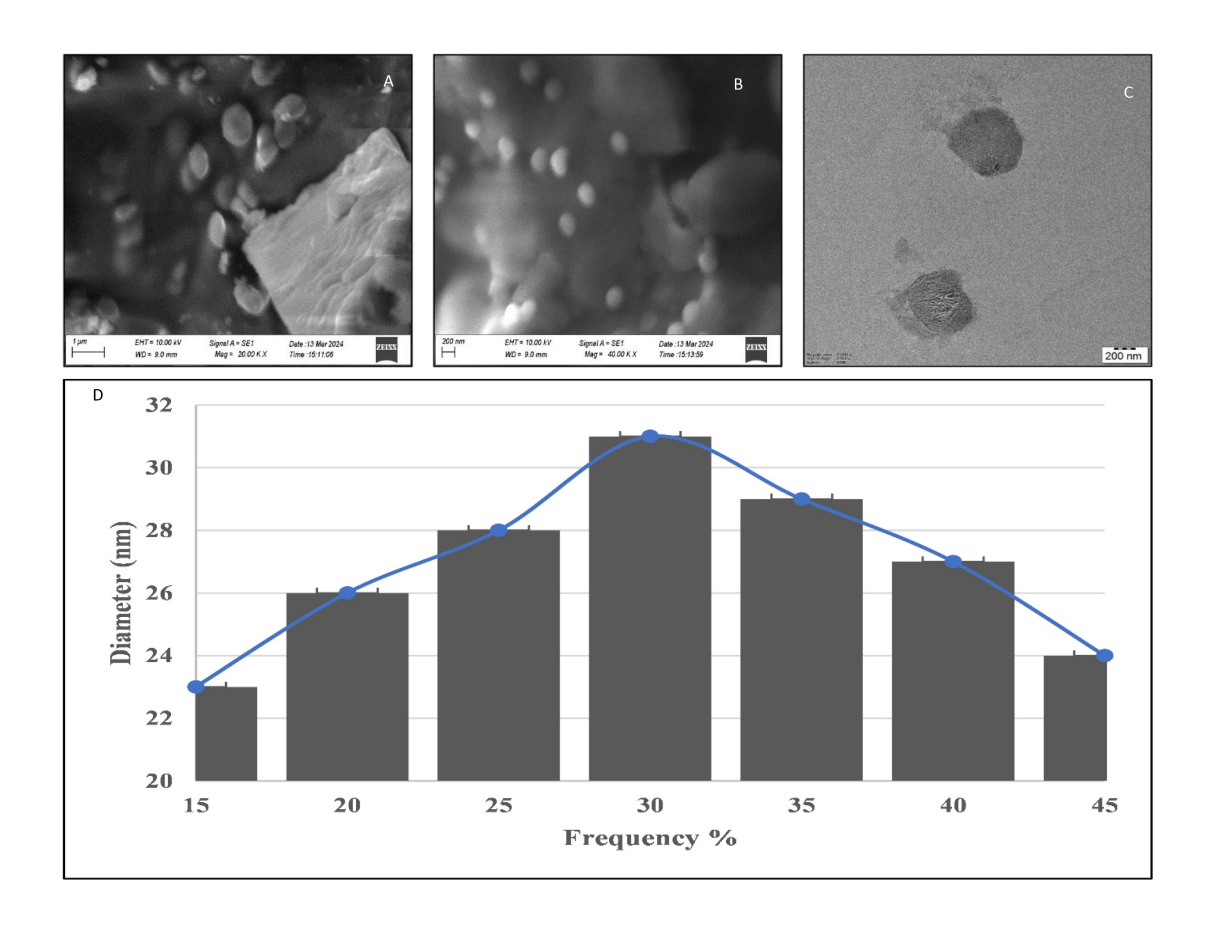


Fig. 5. SEM and TEM analysis of *T. terrestris***-mediated iron nanoparticles.** (A,B) SEM micrograph images in different magnification. Scale bar: 1 µm. (C) TEM image of T. *terrestris*-Fe₃O₄-NPs. Scale bar: 200nm. (D) Size distribution histogram.

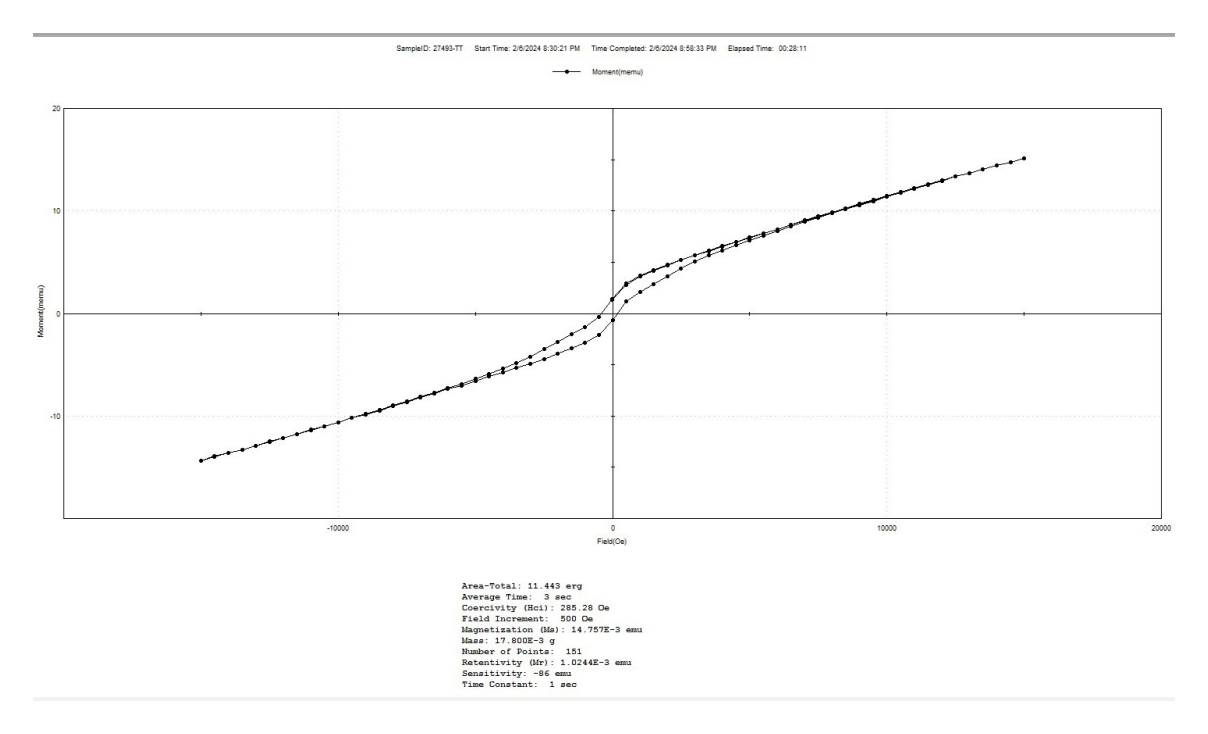


Fig. 6. Magnetic characterization of *T. terrestris*-mediated iron nanoparticles by vibrating sample magnetometry(VSM) technique.



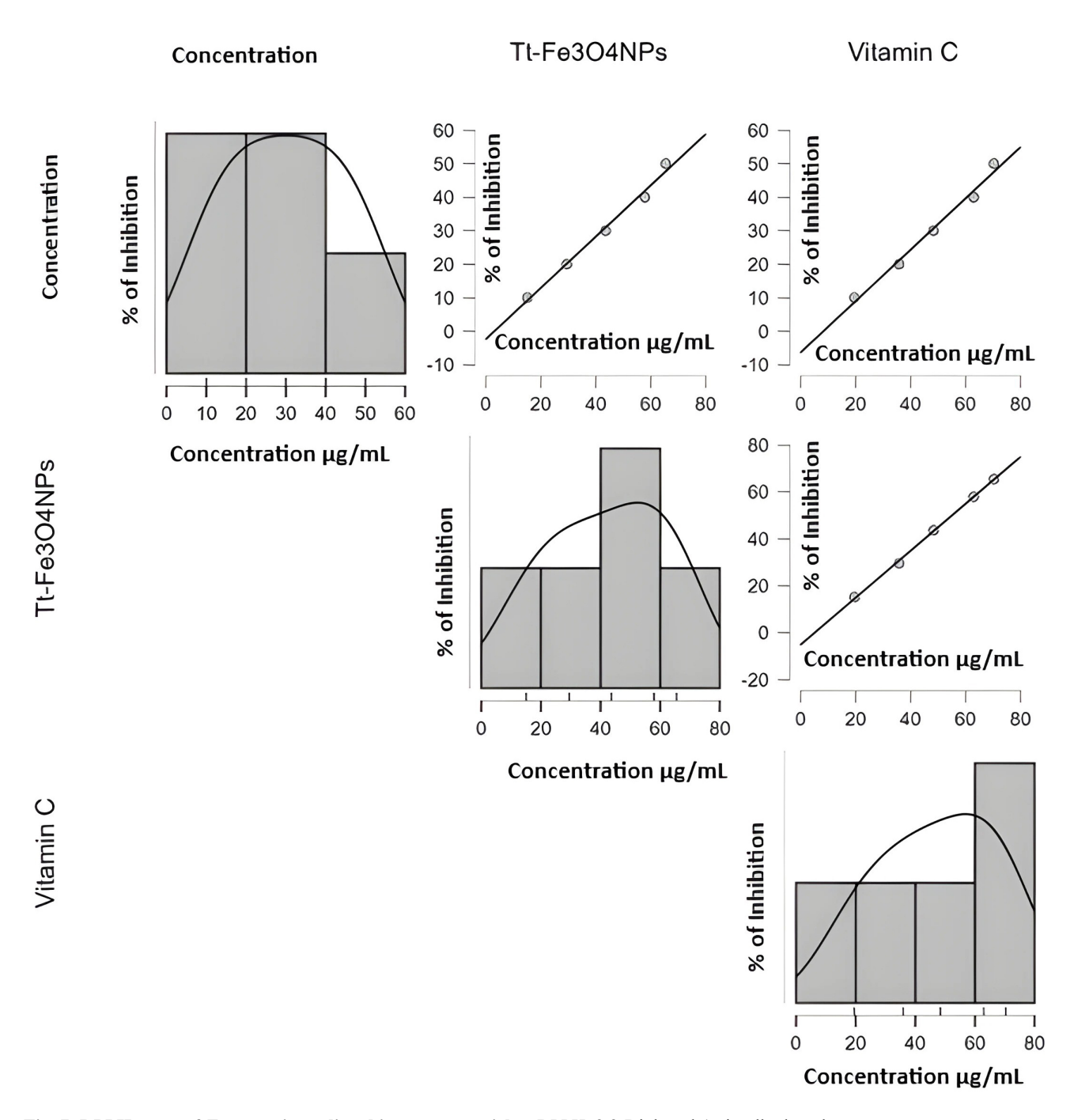


Fig. 7. DPPH assay of T. terrestris-mediated iron nanoparticles. DPPH, 2,2-Diphenyl-1 picrylhydrazyl.

3.6 Anti-Oxidant Activity of T. terrestris-Fe₃O₄-NPs

Free radicals are molecules that are extremely reactive and possess unpaired electrons. They have the potential to cause cellular injury during the metabolic process. This oxidative stress is mitigated by antioxidants, which are recognized for their ability to neutralize these free radicals. Secondary metabolites in plants often exhibit antioxidant properties, despite being non-nutritive, and can benefit human health when consumed [56].

The DPPH and hydrogen peroxide radical assays were employed to evaluate the antioxidant activity of $\it Tribulus$ $\it terrestris-mediated Fe₃O₄-NPs. The Fe₃O₄-NPs effectively.$

tively neutralized free radicals. In the DPPH assay, conducted with doses ranging from 10 to 50 μ g/mL, the Fe₃O₄-NPs demonstrated significant radical-scavenging activity, with a peak inhibition of 65.5% at 50 μ g/mL. For comparison, standard ascorbic acid (Vitamin-C) showed an inhibition of 70.4% at the same concentration, as illustrated in Fig. 7. Nandini and Subhashini [57] reported a DPPH radical scavenging activity of about 61.4% in *Cuminum cyminum*, while Deshmukh *et al.* [58] observed a maximum radical scavenging activity of 60% in *fenugreek* seed-mediated Fe-NPs.



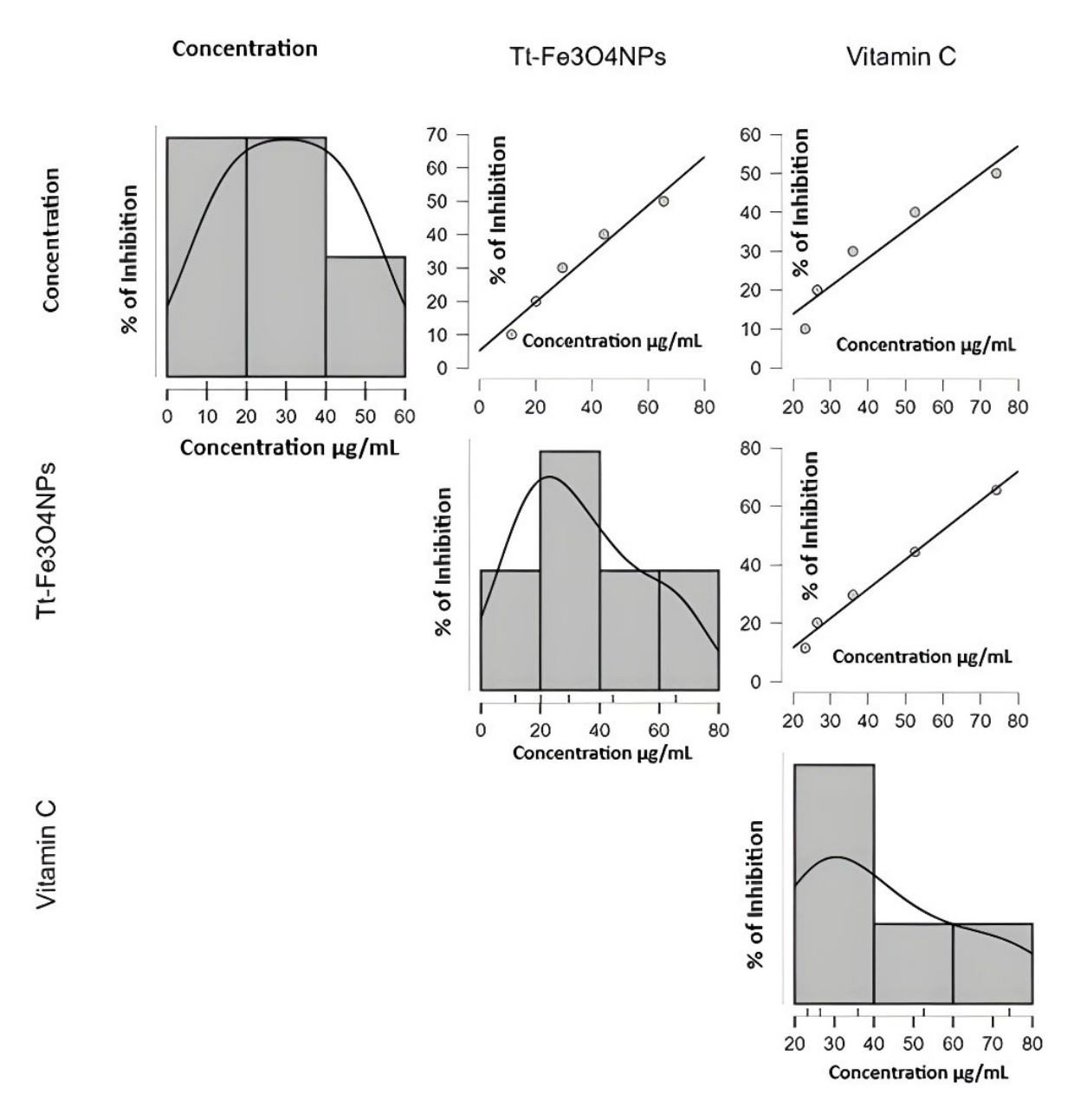


Fig. 8. Hydrogen peroxide assay of *T. terrestris*-mediated iron nanoparticles.

In the hydrogen peroxide assay, *T. terrestris*-Fe₃O₄-NPs exhibited 65.56% inhibition of free radicals at a concentration of 50 µg/mL. Fig. 8 shows that vitamin C suppressed free radicals by 74.23% at the same dose. Essa *et al.* [59] reported a 42.38% scavenging activity for hydrogen peroxide in *Vitis vinifera* leaf-mediated Fe-NPs, while Sandhya and Kalaiselvam [60] observed a 44.12% radical scavenging activity in *Borassus flabellifer* tender seed-synthesized iron nanoparticles. The significant antioxidant activity of *Tribulus terrestris* is attributed to its numerous phenolic hydroxyl groups [61]. Based on Lushchak [62], antioxidants reduce oxidative damage to biological components and restrict cancer cell development by suppressing free radicals.

3.7 Anti-Inflammatory Activity of T. terrestris-Fe₃O₄-NPs

Tribulus terrestris-synthesized Fe₃O₄-NPs demonstrated the capacity to inhibit the denaturation of bovine serum albumin (BSA). At 50 μg/mL, Fe₃O₄-NPs showed maximum inhibition of 43.28. For comparison, the standard drug diclofenac, at the same concentration of 50 μg/mL, achieved a higher inhibition of 54.57%, as shown in Fig. 9. Khuda *et al.* [63] investigated the *in vitro* anti-inflammatory activity of crude extracts from *Xanthium strumarium* and *Achyranthes aspera* leaves, reporting a maximum inhibition of 73%. Additionally, Bailey-Shaw *et al.* [64] studied the anti-inflammatory properties of 99 plant samples. Among these, iron nanoparticles synthesized from *Mangifera indica* (Julie mango) leaves showed a significant inhibition of 72.60%.



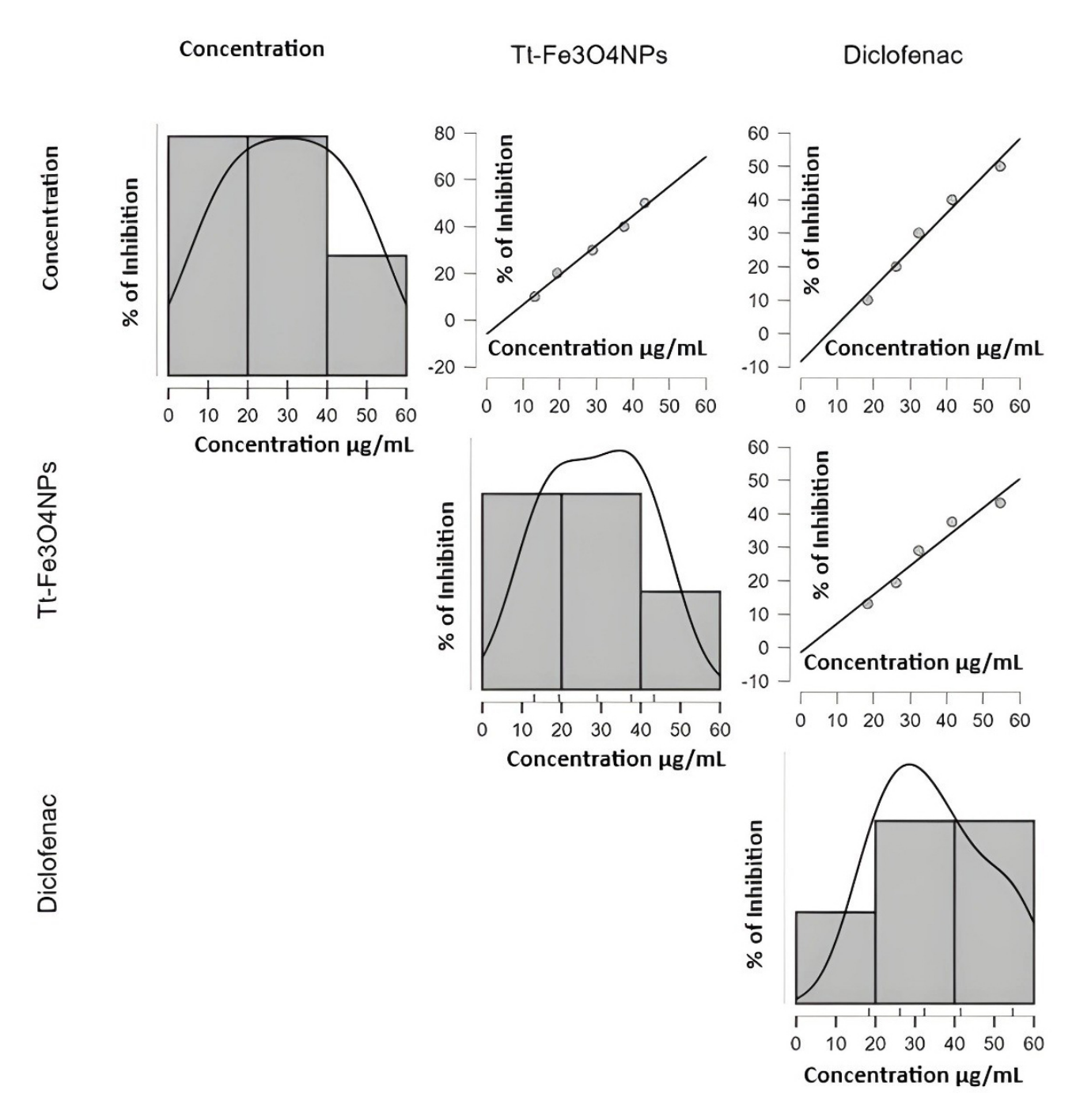


Fig. 9. Protein denaturation assay of *T. terrestris*-mediated iron nanoparticles.

3.8 Antibacterial Activity of T. terrestris-Fe₃O₄-NPs

The antibacterial efficacy of the synthesized nanoparticles is comparable to that of the original *Tribulus terrestris* plant extract. This antimicrobial activity arises because the functional groups from the plant extract, which possess inherent herbal qualities, saturate the nanoparticle surfaces. The nanoparticles' diminutive size enables them to easily pass through the bacterial cell walls, resulting in the demise of the cells [65].

The antibacterial efficacy of the synthesized $\it{T. ter-restris}$ -Fe $_3$ O $_4$ -NPs was evaluated, as illustrated in Fig. 10. At a concentration of 100 μ L, the maximum zones of inhibi-

tion were observed against *Lactobacillus* (35 mm) and *Vibrio cholerae* (34 mm). Moderate inhibition was noted for *Staphylococcus aureus* (19 mm) and *Pseudomonas aeruginosa* (25 mm). The synthesized nanoparticles demonstrated the highest effectiveness against *Lactobacillus*, as illustrated in Fig. 11.

Kanagasubbulakshmi and Kadirvelu [65] reported similar findings for nanoparticles synthesized from *Lagenaria siceraria*. Their study showed that these nanoparticles had comparable antibacterial potential to the plant extract, with higher efficacy against *Staphylococcus aureus* at higher concentrations. At lower concentrations, how-



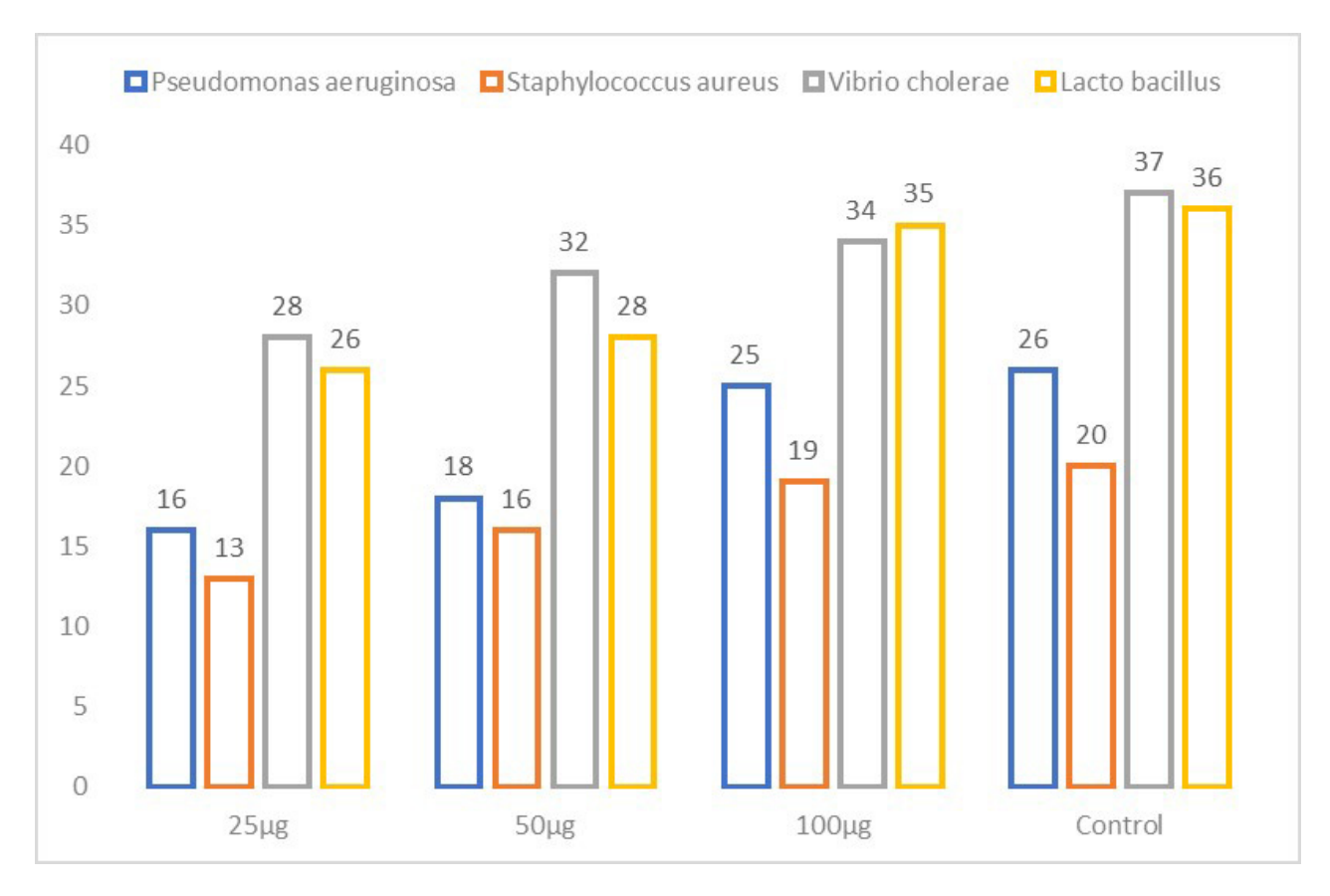


Fig. 10. Antibacterial activity of T. terrestris-mediated iron nanoparticles against wound pathogens.

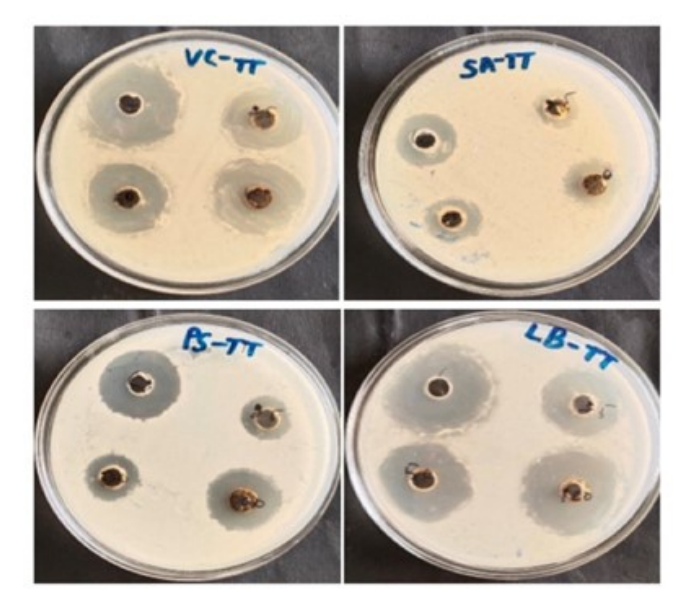


Fig. 11. Zone of inhibition of $\it T. terrestris$ -mediated iron nanoparticles.

ever, the nanoparticles did not show inhibition, as depicted in Fig. 11. Additionally, Yadav *et al.* [66] examined the antibacterial efficiency of *Aloe vera* nanoparticles against *Klebsiella pneumoniae* and reported a 17-mm maximal inhibitory zone.

3.9 Anticancer Activity of T. terrestris-Fe₃O₄-NPs

The MTT method was used to evaluate the *in vitro* anticancer effectiveness of *T. terrestris*-Fe₃O₄-NPs against the HCT-116 colon cancer cell line. The results indicated that higher concentrations of *T. terrestris*-Fe₃O₄-NPs led to a greater percentage of cell inhibition. The half-inhibitory concentration (IC₅₀) for HCT-116 cells was 25.95 μ g/mL,



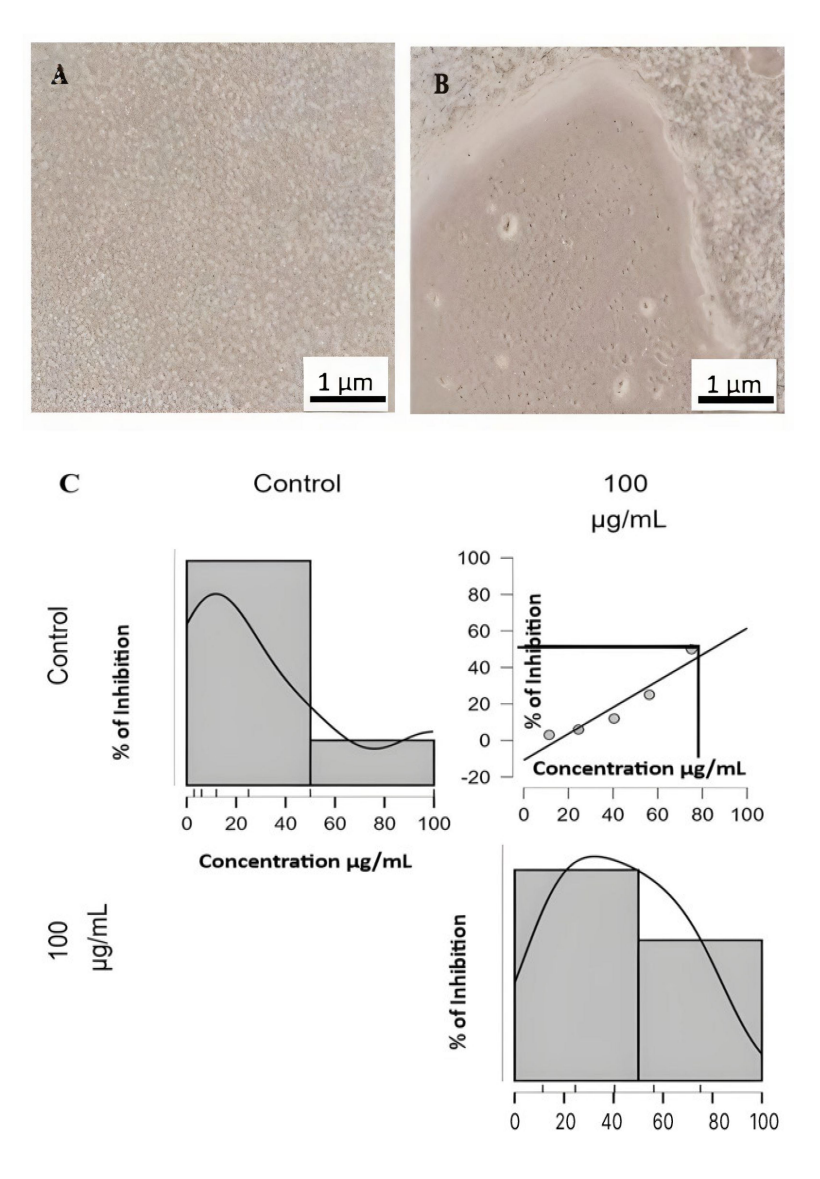


Fig. 12. Cell Viability (A) Control cells (B) Treated Cells (C) Cytotoxic activity of *T. terrestris*-mediated iron nanoparticles in HCT-116 cell line. Scale bar: 1 μm.

as shown in Fig. 12. In contrast, for the MG-63 (osteosarcoma) cell lines, the IC₅₀ value was 35.36 μg/mL, depicted in Fig. 13. Microscopic images of both cell lines reveal that *T. terrestris*-Fe₃O₄-NPs are more effective against colon cancer than bone cancer. According to Alkahtane *et al.* [67] studied the cytotoxicity of the iron oxide nanoparticles on HCT 116 cell lines and it limit proliferation at 55 mg/mL and less toxic for fibroblast cells.

Yusefi *et al.* [68] investigated the cytotoxic effects of Fe₃O₄-NPs maintained with *Garcinia mangostana* fruit peel on HCT-116 and normal CCD112 cell lines. At a dosage of 250 μ g/mL, a 68% suppression of colon cancer cells was observed. Chauhan *et al.* [69] noted that malignant cells, lacking a protective mucus layer, are more susceptible to therapeutic agents like those derived from *T. terrestris*. Based on these cytotoxicity results, further anticancer screening of *T. terrestris*-Fe₃O₄-NPs at concentra-

tions of 50, 25, and 10 µg/mL was deemed necessary. According to Ratan *et al.* [70], plant extracts include biological components that serve as capping and reducing agents in nanoparticles, effectively inhibiting cancer cell development. The dimensions, and morphology of iron nanoparticles are also contributing factors in inducing apoptosis in cancer cells by stimulating the increase of reactive oxygen species (ROS). As per Ansari and Asiri [71], the anticancer mechanism of iron oxide nanoparticles is caused by releasing Fe ions to eliminate cancer cells. It is conceivable that Fe_3O_4 -NPs are responsible for the development of reactive oxygen species, which eradicate malignant cells.

3.10 Wound Healing Assay

The impact of green synthesized *T. terrestris*-Fe₃O₄-NPs on cancer cell migration was evaluated through a wound healing assay using HCT-116 colon cancer cells.



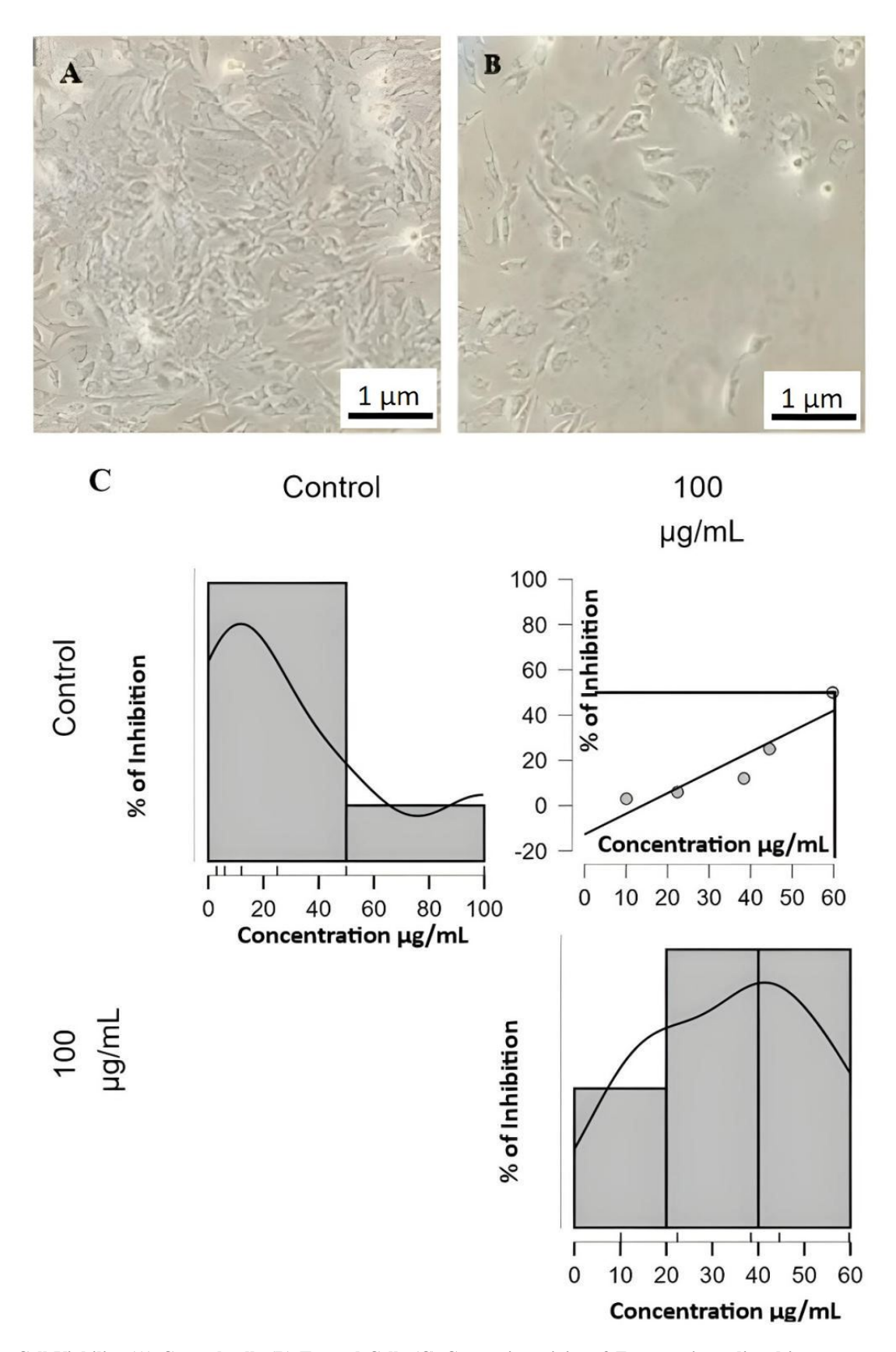


Fig. 13. Cell Viability (A) Control cells (B) Treated Cells (C) Cytotoxic activity of T. terrestris-mediated iron nanoparticles in MG-63 cell line. Scale bar: $1 \mu m$.

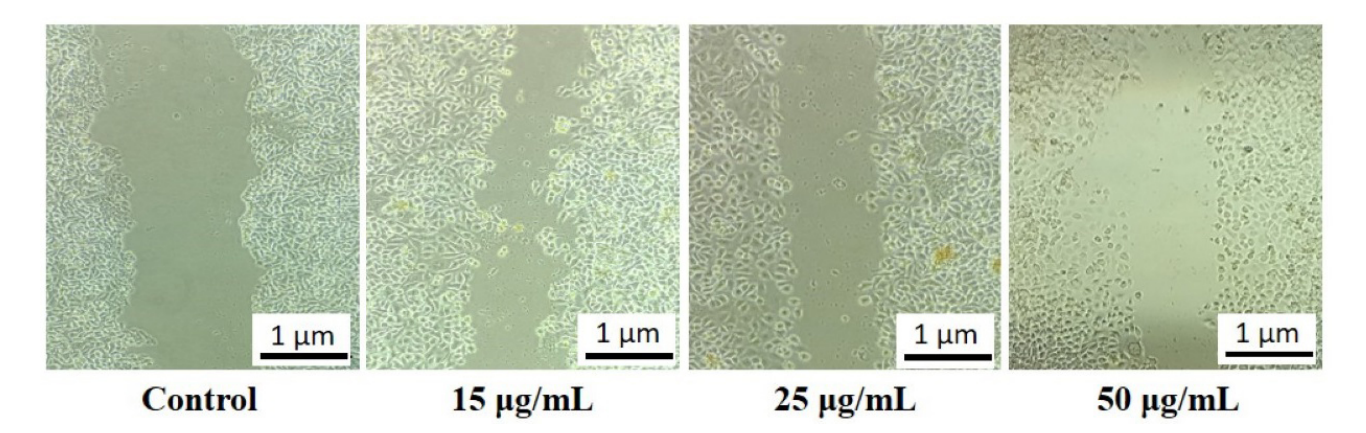


Fig. 14. Wound healing assay of $\it T.$ terrestris-mediated iron nanoparticles. Scale bar: 1 μm .

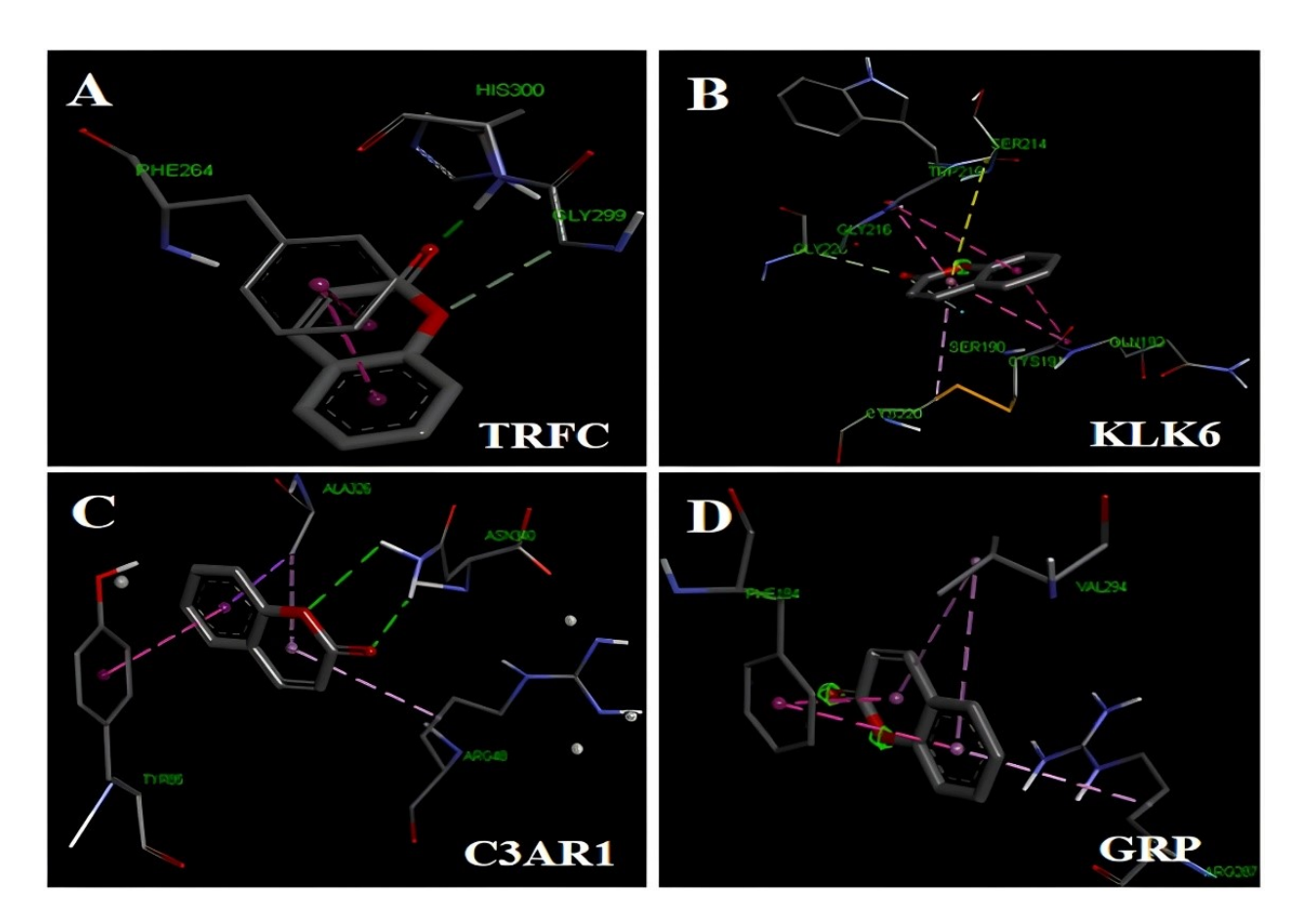


Fig. 15. Molecular interaction between *T. terrestris*-mediated iron nanoparticles derived compounds with Adenomatous polyposis coli (APC) pathway proteins (A) TRFC (B) KLK6 (C) C3AR1 and (D) GRP.

This study showed that *T. terrestris*-Fe $_3$ O₄-NPs at 10, 25, and 50 µg/mL substantially reduced wound closure compared to normal control cells. Notably, at the highest concentration of 50 µg/mL, the migration of HCT-116 cells was reduced by 90%, as illustrated in Fig. 14. This result indicates that the nanoparticles effectively hindered cancer cell migration, in contrast to the untreated control cells, which showed continued migration and spread.

The results underscore the potential of plant-mediated iron nanoparticles in reducing tumor cell migration. Such nanoparticles may enhance wound healing processes by promoting repair mechanisms and collagen synthesis, thereby improving tensile strength [72]. Adnan *et al.* [73] conducted a similar wound closure assay with HCT-116, and A549 cells were treated with an ethanolic extract of *Selaginella repanda*, observing dose-dependent inhibition of cell migration.



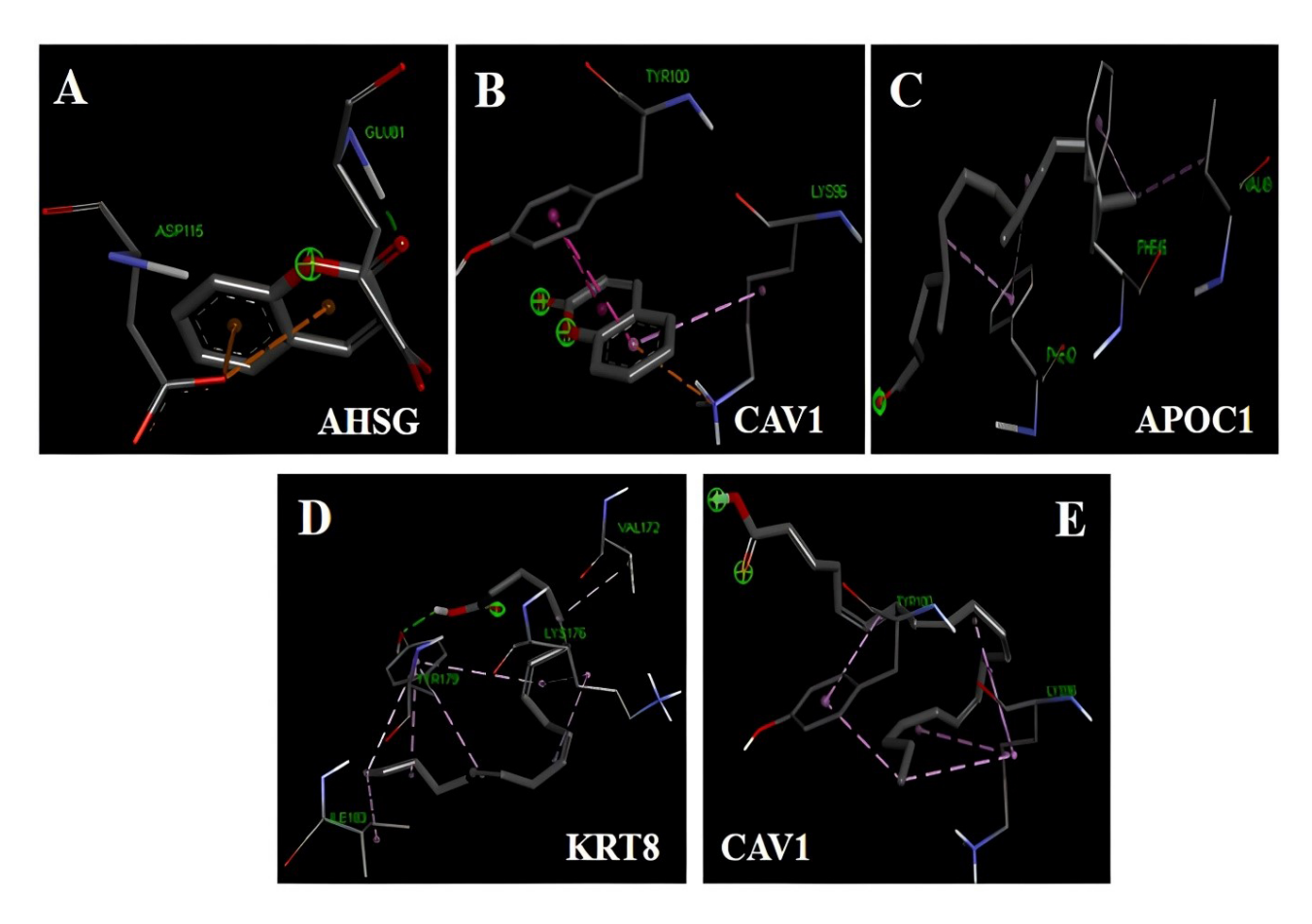


Fig. 16. Molecular interaction between *T. terrestris*-derived compounds with Adenomatous polyposis coli (APC) proteins (A) AHSG, (B) CAV1, (C) APOC1, (D) KRT8, (E) CAV1.

Table 1. Binding affinity between Proteins and Ligands.

Compounds	KRT8	TFRC	KLK6	C3AR1	AHSG	GRP	APOC1	CAV1
Stearic acid	-3.5	-4.8	-4.6	-4.5	-4.4	-5.5	-4	-3.8
2-Hexanol,2-Methyl	-3.1	-4.3	-4.3	-3.6	-3.9	-4.9	-3.5	-3.2
Hexa decanoic acid	-3.3	-5.7	-4.8	-4.3	-4	-5.6	-3.9	-3.7
Octadecanoic acid	-3.4	-5.1	-4.2	-4.4	-3.1	-5.6	-3.9	-3.8
2-Pentadecanone	-3.7	-5.8	-4.3	-4.8	-4.8	-5.7	-4.7*	-4.7
Coumaric acid	-3.5	-6.2*	-6*	-6*	-5.6*	-6.8*	-4.1	-4.8*
Benzofuran	-3.6	-5.2	-5	-5.9	-5	-5.6	-3.5	-4.3
Archidic acid	-4.1*	-5.8	-4.8	-5.3	-4.1	-6.7	-4.4	-4.8
5 Fluorouracil**	-3.5	-5.1	-5.2	-4.8	-4.3	-5	-3.7	-3.6

^{**} Standard drug and * Highest binding affinity.

3.11 Molecular Docking

The command-line software utilized in this study divided the docking results into an output registry in PDB format and a log file in text format. Given the frequent abnormalities in the Adenomatous Polyposis Coli (APC) pathway in colon cancer, which underscores its significance in colon cancer development [74], the docking analysis was centered on proteins associated with the APC pathway. Binding affinity values derived from molecular docking investigations are outlined in Table 1. The results indicated that coumaric acid effectively targets several proteins involved

in colon cancer, including KRT8, TFRC, KLK6, C3AR1, AHSG, GRP, APOC1, and CAV1, with 5-Fluorouracil used as a standard drug for comparison. Figs. 15,16 highlight that coumaric acid demonstrated the highest binding affinities with GRP (6.8), TFRC (6.2), KLK6 (6), and C3AR1 (6) proteins. These results suggest that coumaric acid exhibits substantial binding affinity towards key proteins associated with colon cancer, as evidenced by these bioinformatics analyses. Zhang *et al.* [75] also investigated the binding affinity of ginger compounds with colon cancer proteins using *in silico* methods. They found that the



targeted proteins TP53, HSP90AA1, and JAK2 exhibited stronger interactions with ginger compounds compared to prototype ligands, supporting the efficacy of targeted therapeutic approaches.

4. Conclusion

The green synthesized T. terrestris-Fe₃O₄-NPs are environmentally safe and pose no significant risks. Various characterization techniques were performed, such as UV spectroscopy, FTIR, XRD, SEM, TEM, and VSM. The Tt-Fe₃O₄-NPs demonstrated significant antioxidants, which is one of the main components required for DNA repair in the etiology of cancer. A lot of anticancer drugs work by inhibiting cancer cells through antioxidants. Many cancer cells are infected by microorganisms in advanced stages so the eradication of microorganisms from cancer cells, clinically is very challenging. Currently, only a few antibiotics are capable of killing microorganisms and cancer cells. The Tt-Fe₃O₄-NPs were able to kill the microorganism growth, which was confirmed through antimicrobial activity. Some of the toxic chemicals in the body cause inflammation, and normal cells are converted into cancer cells through inflammation. The synthesized nanoparticle has anti-inflammatory activity, as demonstrated by an antiinflammation assay. Generally, normal cells have inflammation from some of the foreign agents and its converted cancer cells which is followed by microorganism infection. when normal cells have a deficiency of antioxidant capacity in the body to form inflammation, infection, and cancer. T. terrestris also exhibited notable anticancer efficacy against colon cancer cell lines through anticancer activity and scratch assays. The bioactive compound coumaric acid strongly binds to key proteins linked to colon cancer, such as TRFC, KLK6, C3AR1, and GRP, as shown by molecular docking studies. It also contains many secondary metabolites that interact with colon cancer protein markers. As a result, it is suggested that our nanoparticles can modulate the colon cancer signaling pathway. In this study, we confirmed our plant has anti-inflammation, antimicrobial, and anticancer activity, which is necessary for any anticancer drug. So, we believe this drug may be very optimum for colon cancer patients. This drug will be used in clinical trials in our future studies.

Availability of Data and Materials

The datasets used and/or analyzed during the current study are available from the corresponding author on reasonable request.

Author Contributions

Conceptualization: TP, GB, BKR; Methodology: RR, HS, GB; Analysis and interpretation of data: MG, SK; Data curations: MN, MRAW; writing-original draft preparation: RR; Writing-review and editing, interpretation of data: TP, MR; Visualization: TP, AS, RA; Supervision and data cu-

ration: TP, BKR, MR, SK, AS, WHA. All authors have participated sufficiently in the work to take public responsibility for appropriate portions of the content and agreed to be accountable for all aspects of the work in ensuring that questions related to its accuracy or integrity. All authors contributed to editorial changes in the manuscript. All authors read and approved the final manuscript.

Ethics Approval and Consent to Participate

Tribulus terrestris (Tt) was used in this study. It is a flowering plant with yellow flowers. The plant was collected from Pudhur and its surrounding areas in Chennai. It was identified as 387.1753 and authenticated by the Siddha Central Research Institute in Chennai.

Acknowledgment

We gratefully acknowledge Er. A.C.S. Arun Kumar, President, Dr. M.G.R. Educational and Research Institute, for providing the necessary facilities, and we acknowledge the Nanotechnology Research Centre (NRC), SRMIST, for providing an instrumentation facility for nanoparticle characterization. We would like to acknowledge the Researchers Supporting Project Number (RSP2025R293), King Saud University, Riyadh, Saudi Arabia.

Funding

This work was funded by the Researchers Supporting Project Number (RSP2025R293), King Saud University, Riyadh, Saudi Arabia.

Conflict of Interest

The authors declare no conflict of interest.

References

- [1] Dimri GP. What has senescence got to do with cancer? Cancer Cell. 2012; 7: 505–512. https://doi.org/10.1016/j.ccr.2005.05.
- [2] Stratton MR, Campbell PJ, Futreal PA. The cancer genome. Nature. 2009; 458: 719–724. https://doi.org/10.1038/nature07943.
- [3] Labianca R, Beretta GD, Kildani B, Milesi L, Merlin F, Mosconi S, et al. Colon cancer. Critical Reviews in Oncology/hematology. 2010; 74: 106–133. https://doi.org/10.1016/j. critrevonc.2010.01.010.
- [4] Cheng J, Wang X, Qiu L, Li Y, Marraiki N, Elgorban AM, et al. Green synthesized zinc oxide nanoparticles regulates the apoptotic expression in bone cancer cells MG-63 cells. Journal of Photochemistry and Photobiology. B, Biology. 2020; 202: 111644. https://doi.org/10.1016/j.jphotobiol.2019.111644.
- [5] El-Kassas HY, El-Sheekh MM. Cytotoxic activity of biosynthesized gold nanoparticles with an extract of the red seaweed Corallina officinalis on the MCF-7 human breast cancer cell line. Asian Pacific Journal of Cancer Prevention: APJCP. 2014; 15: 4311–4317. https://doi.org/10.7314/apjcp.2014.15.10.4311.
- [6] Logothetidis, S. Nanotechnology: Principles and Applications. Nanostructured Materials and Their Applications. NanoScience and Technology (ed.) (pp. 1-22). Springer: Berlin, Heidelberg. 2012. https://doi.org/10.1007/978-3-642-22227-6_1.



- [7] Ramsden JJ. What is nanotechnology? Nanotechnology Perceptions. 2005; 1: 3–17.
- [8] Mansoori GA, Soelaiman TF. Nanotechnology–An introduction for the standards community. ASTM International. 2005; 2.
- [9] Khan I, Saeed K, Khan I. Nanoparticles: Properties, applications, and toxicities. Arabian Journal of Chemistry. 2019 12: 908–931. https://doi.org/10.1016/j.arabjc.2017.05.011.
- [10] Biswas P, Wu CY. Nanoparticles and the environment. Journal of the Air & Waste Management Association (1995). 2005; 55: 708–746. https://doi.org/10.1080/10473289.2005.10464656.
- [11] Ilinskaya AN, Dobrovolskaia MA. Nanoparticles and the blood coagulation system. Part I: benefits of nanotechnology. Nanomedicine (London, England). 2013; 8: 773–784. https://doi.org/10.2217/nnm.13.48.
- [12] Roncaglioni A, Toropov AA, Toropova AP, Benfenati E. In silico methods to predict drug toxicity. Current Opinion in Pharmacology. 2013; 13: 802–806. https://doi.org/10.1016/j.coph.2013.06.001.
- [13] Kaushik J, Tandon S, Gupta V, Nayyar J, Singla SK, Tandon C. Response surface methodology based extraction of Tribulus terrestris leads to an upsurge of antilithiatic potential by inhibition of calcium oxalate crystallization processes. PloS One. 2017; 12: e0183218. https://doi.org/10.1371/journal.pone.0183218.
- [14] Yan W, Lien HL, Koel BE, Zhang WX. Iron nanoparticles for environmental clean-up: recent developments and future outlook. Environmental Science. Processes & Impacts. 2013; 15: 63–77. https://doi.org/10.1039/c2em30691c.
- [15] Fahmy HM, Mohamed FM, Marzouq MH, Mustafa ABED, Alsoudi AM, Ali, *et al.* Review of green methods of iron nanoparticle synthesis and applications. Bio NanoScience. 2018; 8: 491–503.
- [16] Harshiny M, Iswarya CN, Matheswaran M. Biogenic synthesis of iron nanoparticles using Amaranthus dubius leaf extract as a reducing agent. Powder Technology. 2015; 286: 744–749.
- [17] Ghosh VK, Bhope SG, Kuber VV, Sagulale AD. An improved method for the extraction and quantitation of diosgenin in Tribulus terrestris L. Journal of Liquid Chromatography & Related Technologies. 2012; 35: 1141–1155.
- [18] Chhatre S, Nesari T, Somani G, Kanchan D, Sathaye S. Phytopharmacological overview of Tribulus terrestris. Pharmacognosy Reviews. 2014; 8: 45–51. https://doi.org/10.4103/0973-7847.125530.
- [19] Zhu W, Du Y, Meng H, Dong Y, Li L. A review of traditional pharmacological uses, phytochemistry, and pharmacological activities of Tribulus terrestris. Chemistry Central Journal. 2017; 11: 60. https://doi.org/10.1186/s13065-017-0289-x.
- [20] Aryal S, Kuwar P, Thapa C. Antiurolithiatic activity of selected plant extracts against calcium oxalate crystals. Journal of Medicinal Plants Research. 2021; 15: 172-177.
- [21] Solowey E, Lichtenstein M, Sallon S, Paavilainen H, Solowey E, Lorberboum-Galski H. Evaluating medicinal plants for anticancer activity. TheScientificWorldJournal. 2014; 2014: 721402. https://doi.org/10.1155/2014/721402.
- [22] Kooti W, Servatyari K, Behzadifar M, Asadi-Samani M, Sadeghi F, Nouri B, et al. Effective Medicinal Plant in Cancer Treatment, Part 2: Review Study. Journal of Evidence-based Complementary & Alternative Medicine. 2017; 22: 982–995. https://doi.org/10.1177/2156587217696927.
- [23] Zhao P, El-kott A, Ahmed AE, Khames A, Zein MA. Green synthesis of gold nanoparticles (Au NPs) using Tribulus terrestris extract: Investigation of its catalytic activity in the oxidation of sulfides to sulfoxides and study of its anti-acute leukemia activity. Inorganic Chemistry Communications. 2021; 131: 108781.
- [24] Ansari SH, Islam F, Sameem M. Influence of nanotechnology on herbal drugs: A Review. Journal of Advanced Pharmaceutical Technology & Research. 2012; 3: 142–146. https://doi.org/10. 4103/2231-4040.101006.

- [25] Alrabie A, Alrabie NA, Saeedy M. ICP-MS analysis, GC-MS identification of antimicrobial, Antioxidant, and Antidiabetic volatile bioactive constituents from Tribulus terrestris fruits. World Journal of Pharmacy and Pharmaceutical Sciences. 2022; 12: 1415–1429.
- [26] Sadhasivam S, Vinayagam V, Balasubramaniyan M. Recent advancement in the biogenic synthesis of iron nanoparticles. Journal of Molecular Structure. 2020; 1217: 128372.
- [27] Akash MSH, Rehman K, Akash MSH, Rehman K. Ultravioletvisible (UV-VIS) spectroscopy. Essentials of Pharmaceutical Analysis. 2020; 29–56.
- [28] Hussain A, Yasar M, Ahmad G, Ijaz M, Aziz A, Nawaz MG, et al. Synthesis, characterization, and applications of iron oxide nanoparticles. International Journal of Health Sciences. 2023; 17: 3–10.
- [29] Velsankar K, Parvathy G, Mohandoss S, Krishna Kumar M, Sudhahar S. Celosia argentea leaf extract-mediated green synthesized iron oxide nanoparticles for bio-applications. Journal of Nanostructure in Chemistry. 2021; 12: 1–16.
- [30] Bharathi D, Preethi S, Abarna K, Nithyasri M, Kishore P, Deepika K. Bio-inspired synthesis of flower shaped iron oxide nanoparticles (FeONPs) using phytochemicals of Solanum ly-copersicum leaf extract for biomedical applications. Biocatalysis and Agricultural Biotechnology. 2020; 27: 101698.
- [31] Mishra D, Arora R, Lahiri S, Amritphale SS, Chandra. Synthesis and characterization of iron oxide nanoparticles by solvothermal method. Protection of Metals and Physical Chemistry of Surfaces. 2014; 50: 628–631.
- [32] Abegunde SM, Idowu KS, Sulaimon AO. Plant-mediated iron nanoparticles and their applications as adsorbents for water treatment—a review. Journal of Chemical Reviews. 2020; 2: 103–113
- [33] Asadujjaman M, Hossain MA, Karmakar UK. Assessment of DPPH free radical scavenging activity of some medicinal plants. Pharmacology online. 2013; 1: 161–165.
- [34] Keser S, Celik S, Turkoglu S, Yilmaz O, Turkoglu I. Hydrogen peroxide radical scavenging and total antioxidant activity of hawthorn. Chemistry Journal. 2012; 2: 9–12.
- [35] Sultana MJ, Nibir AIS, Ahmed, F.R.S. Biosensing and antiinflammatory effects of silver, copper and iron nanoparticles from the leaf extract of Catharanthus roseus. Beni-Suef University Journal of Basic and Applied Sciences. 2023; 12: 26.
- [36] Ababutain IM. Antimicrobial activity of ethanolic extracts from some medicinal plants. Australian Journal of Basic and Applied Sciences. 2011; 5: 678–683.
- [37] Kai K, Nagano O, Sugihara E, Arima Y, Sampetrean O, Ishimoto T, et al. Maintenance of HCT116 colon cancer cell line conforms to a stochastic model but not a cancer stem cell model. Cancer Science. 2009; 100: 2275–2282. https://doi.org/10.1111/j. 1349-7006.2009.01318.x.
- [38] Florento L, Matias R, Tuaño E, Santiago K, Dela Cruz F, Tuazon A. Comparison of Cytotoxic Activity of Anticancer Drugs against Various Human Tumor Cell Lines Using In Vitro Cell-Based Approach. International Journal of Biomedical Science: IJBS, 2012; 8: 76–80.
- [39] Bouabdallah S, Azzouz R, Al-Khafaji K, Ben-Attia, M. Investigating flavonoids derived from Tribulus terrestris L. as prospective candidates for Alzheimer's disease treatment: Molecular docking modeling of their interactions with physiological system receptors. Journal of Bioresources and Environmental Sciences. 2024; 3: 93–100
- [40] Naqvi AAT, Mohammad T, Hasan GM, Hassan MI. Advancements in Docking and Molecular Dynamics Simulations Towards Ligand-receptor Interactions and Structure-function Relationships. Current Topics in Medicinal Chemistry. 2018; 18: 1755–1768.



- https://doi.org/10.2174/1568026618666181025114157.
- [41] Ibrahim NM and Kadhim EJ. Phytochemical investigation, antioxidant activity of Iraqi Tribulus terrestris. Iraqi Journal of Pharmaceutical Sciences. 2015; 24: 68–73.
- [42] Asghar MA, Zahir E, Shahid SM, Khan MN, Asghar MA, Iqbal J. et al. Iron, copper, and silver nanoparticles: Green synthesis using green and black tea leaves extracts and evaluation of antibacterial, antifungal and aflatoxin B1 adsorption activity. LWT. 2018; 90: 98–107. https://doi.org/10.1016/j.lwt.2017.12.009.
- [43] Pattanayak M, Nayak PL. Eco-friendly green synthesis of iron nanoparticles from various plants and spices extract. International Journal of Plant, Animal and Environmental Sciences. 2013; 3: 68–78.
- [44] Rajiv P, Bavadharani B, Kumar MN, Vanathi P. Synthesis and characterization of biogenic iron oxide nanoparticles using a green chemistry approach and evaluating their biological activities. Biocatalysis and Agricultural Biotechnology. 2017; 12: 45– 49
- [45] Kamboj VP. Herbal medicine. Current Science. 2000; 78: 35–39.
- [46] Rajendran SP, Sengodan K. Synthesis and characterization of zinc oxide and iron oxide nanoparticles using Sesbania grandiflora leaf extract as a reducing agent. Journal of Nanoscience. 2017; 2017: 8348507. https://doi.org/10.1155/2017/8348507.
- [47] Pallela PNVK, Ummey S, Ruddaraju LK, Gadi S, Cherukuri CS, Barla S, et al. Antibacterial efficacy of green synthesized α-Fe₂O₃ nanoparticles using Sida cordifolia plant extract. Heliyon. 2019; 5: e02765. https://doi.org/10.1016/j.heliyon.2019.e02765
- [48] Dhuper S, Panda D, Nayak PL. Green synthesis and characterization of zero valent iron nanoparticles from the leaf extract of Mangifera indica. Nano Trends: A Journal of Nanotechnology and Its Applications. 2012; 13: 16–22.
- [49] Patil YY, Sutar VB, Tiwari AP. Green synthesis of magnetic iron nanoparticles using medicinal plant tridax procumbens leaf extracts and its application as an antimicrobial agent against E. coli. International Journal of Applied Pharmaceutics. 2020; 12: 3439.
- [50] Tian C, Chang Y, Zhang Z, Wang H, Xiao S, Cui C, et al. Extraction technology, component analysis, antioxidant, antibacterial, analgesic and anti-inflammatory activities of flavonoids fraction from *Tribulus terrestris* L. leaves. Heliyon. 2019; 5: e02234. https://doi.org/10.1016/j.heliyon.2019.e02234.
- [51] Baskar G, Palaniyandi T, Ravi M, Viswanathan S, Wahab MRA, Surendran H, et al. Biosynthesis of iron oxide nanoparticles from red seaweed Hypnea valentiae and evaluation of their antioxidant and antitumor potential via the AKT/PI3K pathway. Process Biochemistry. 2024; 141: 155–169. https://doi.org/10. 1016/j.procbio.2024.03.010.
- [52] Naseem T, Farrukh MA. Antibacterial activity of green synthesis of iron nanoparticles using Lawsonia inermis and Gardenia jasminoides leaves extract. Journal of Chemistry. 2015; 2015: 912342. https://doi.org/10.1155/2015/912342
- [53] Kheshtzar R, Berenjian A, Taghizadeh SM, Ghasemi Y, Asad AG, Ebrahiminezhad A. Optimization of reaction parameters for the green synthesis of zero-valent iron nanoparticles using pine tree needles. Green Processing and Synthesis. 2019; 8: 846–855.
- [54] Mahdavi M, Namvar F, Ahmad MB, Mohamad R. Green biosynthesis and characterization of magnetic iron oxide (Fe₃O₄) nanoparticles using seaweed (Sargassum muticum) aqueous extract. Molecules (Basel, Switzerland). 2013; 18: 5954–5964. https://doi.org/10.3390/molecules18055954.
- [55] Izadiyan Z, Shameli K, Miyake M, Hara H, Mohamad SEB, Kalantari K, et al. Cytotoxicity assay of plant-mediated synthesized iron oxide nanoparticles using Juglans regia green husk extract. Arabian Journal of Chemistry. 2020; 13: 2011–2023.

- https://doi.org/10.1016/j.arabjc.2018.02.019.
- [56] Nwozo OS, Effiong EM, Aja PM, Awuchi G. Antioxidant, phytochemical, and therapeutic properties of medicinal plants A review. International Journal of Food Properties. 2023; 26: 359–388. https://doi.org/10.1080/10942912.2022.2157425.
- [57] Nandini T, Subhashini D. Antioxidant efficacy of Iron Nanoparticles from aqueous seed extract of Cuminum cyminum. International Journal of Pharm Tech Research. 2015; 8: 19–25.
- [58] Deshmukh AR, Gupta A, Kim BS. Ultrasound Assisted Green Synthesis of Silver and Iron Oxide Nanoparticles Using Fenugreek Seed Extract and Their Enhanced Antibacterial and Antioxidant Activities. BioMed Research International. 2019; 2019: 1714358. https://doi.org/10.1155/2019/1714358.
- [59] Essa RH, Mahmood M, Ahmed SH. Evaluation, antioxidant, antimitotic, and anticancer activity of iron nanoparticles prepared by using water extract of Vitis vinifera L. leaves. Journal of Advanced Laboratory Research in Biology. 2017; 8: 67–73
- [60] Sandhya J, Kalaiselvam S. Biogenic synthesis of magnetic iron oxide nanoparticles using inedible borassus flabellifer seed coat: characterization, antimicrobial, antioxidant activity and in vitro cytotoxicity analysis. Materials Research Express. 2020; 7: 015045.
- [61] Rahman A, Rehman G, Shah N, Hamayun M, Ali S, Ali A, et al. Biosynthesis and Characterization of Silver Nanoparticles Using *Tribulus terrestris* Seeds: Revealed Promising Antidiabetic Potentials. Molecules (Basel, Switzerland). 2023; 28: 4203. https://doi.org/10.3390/molecules28104203.
- [62] Lushchak VI. Free radicals, reactive oxygen species, oxidative stress and its classification. Chemico-biological Interactions. 2014; 224: 164–175. https://doi.org/10.1016/j.cbi.2014.10.016.
- [63] Khuda F, Iqbal Z, Khan A, Zakiullah, Shah Y, Ahmad L, et al. Evaluation of anti-inflammatory activity of selected medicinal plants of Khyber Pakhtunkhwa, Pakistan. Pakistan Journal of Pharmaceutical Sciences. 2014; 27: 365–368.
- [64] Bailey-Shaw YA, Williams LA, Green CE, Rodney S, Smith AM. In-vitro evaluation of the anti-inflammatory potential of selected Jamaican plant extracts using the bovine serum albumin protein denaturation assay. International Journal of Pharmaceutical Sciences Review and Research. 2017; 47: 145–153.
- [65] Kanagasubbulakshmi S, Kadirvelu K. Green synthesis of iron oxide nanoparticles using Lagenaria siceraria and evaluation of its antimicrobial activity. Defence Life Science Journal. 2017; 2: 422–427.
- [66] Yadav JP, Kumar S, Budhwar L, Yadav A, Yadav, M. Characterization and antibacterial activity of synthesized silver and iron nanoparticles using Aloe vera. Journal of Nanomedicine and Nanotechnology. 2016; 7: 2.
- [67] Alkahtane AA, Alghamdi HA, Aljasham AT, Alkahtani S. A possible theranostic approach of chitosan-coated iron oxide nanoparticles against human colorectal carcinoma (HCT-116) cell line. Saudi Journal of Biological Sciences. 2022; 29: 154–160. https://doi.org/10.1016/j.sjbs.2021.08.078.
- [68] Yusefi M, Shameli K, Su Yee O, Teow SY, Hedayatnasab Z, Jahangirian H, et al. Green Synthesis of Fe₃O₄ Nanoparticles Stabilized by a Garcinia mangostana Fruit Peel Extract for Hyperthermia and Anticancer Activities. International Journal of Nanomedicine. 2021; 16: 2515–2532. https://doi.org/10.2147/ LJN.S284134.
- [69] Chauhan S, Sharma D, Goel HC. An in vitro evaluation of Tribulus terrestris L59fruit extract for exploring therapeutic potential against certain gut ailments. Indian Journal of Experimental Biology. 2018; 56: 444–450.
- [70] Ratan ZA, Haidere MF, Nurunnabi M, Shahriar SM, Ahammad AJS, Shim YY, et al. Green Chemistry Synthesis of Silver Nanoparticles and Their Potential Anticancer Effects. Cancers. 2020; 12: 855. https://doi.org/10.3390/cancers12040855.



- [71] Ansari MA, Asiri SMM. Green synthesis, antimicrobial, antibiofilm and antitumor activities of superparamagnetic γ-Fe₂O₃ NPs and their molecular docking study with cell wall mannoproteins and peptidoglycan. International Journal of Biological Macromolecules. 2021; 171: 44–58. https://doi.org/10.1016/j.ijbiomac.2020.12.162.
- [72] Sharma Y, Jeyabalan G, Singh, R. Potential wound healing agents from medicinal plants: a review. Pharmacologia. 2013; 4: 349–358.
- [73] Adnan M, Siddiqui AJ, Hamadou WS, Snoussi M, Badraoui R, Ashraf SA, et al. Deciphering the Molecular Mechanism Responsible for Efficiently Inhibiting Metastasis of Human Non-Small Cell Lung and Colorectal Cancer Cells Targeting
- the Matrix Metalloproteinases by *Selaginella repanda*. Plants (Basel, Switzerland). 2021; 10: 979. https://doi.org/10.3390/pl ants10050979.
- [74] Roh H, Green DW, Boswell CB, Pippin JA, Drebin JA. Suppression of beta-catenin inhibits the neoplastic growth of APC-mutant colon cancer cells. Cancer Research. 2001; 61: 6563–6568.
- [75] Zhang MM, Wang D, Lu F, Zhao R, Ye X, He L, et al. Identification of the active substances and mechanisms of ginger for the treatment of colon cancer based on network pharmacology and molecular docking. BioData Mining. 2021; 14: 1. https://doi.org/10.1186/s13040-020-00232-9.

